NASA CONTRACTOR REPORT

NASA CR-2404

NASA CR-2404

ELECTROMAGNETIC AND SCALAR DIFFRACTION BY A RIGHT-ANGLED WEDGE WITH A UNIFORM SURFACE IMPEDANCE

by Y. M. Hwang

Prepared by
THE OHIO STATE UNIVERSITY
ELECTROSCIENCE LABORATORY
Columbus, Ohio 43212
for Langley Research Center

NATIONAL AERONAUTICS AND SPACE ADMINISTRATION • WASHINGTON, D. C. • MAY 1974

1. Report No.	2. Government Accession No.	3. Recipient's Catalog No.
NASA CR-2404		

4. Title and Subtitle	5. Report Date
ELECTROMAGNETIC AND SCALAR DIFFRACTION BY A RIGHT-ANGLED WEDGE WITH A UNIFORM SURFACE IMPEDANCE	May 1974
	6. Performing Organization Code

7. Author(s)	8. Performing Organization Report No.
Y. M. Hwang	TR 3001-6
	10. Work Unit No. 502-33-13-02

9. Performing Organization Name and Address	11. Contract or Grant No.
The Ohio State University ElectroScience Laboratory Columbus, Ohio 43212	NGR 36-008-144
	13. Type of Report and Period Covered Contractor Report

12. Sponsoring Agency Name and Address	14. Sponsoring Agency Code
National Aeronautics and Space Administration Washington, D.C. 20546	

15. Supplementary Notes

Topical report

16. Abstract

The diffraction of an electromagnetic wave by a perfectly-conducting right-angled wedge with one surface covered by a dielectric slab or absorber is considered. The effect of the coated surface is approximated by a uniform surface impedance. The solution of the normally incident electromagnetic problem is facilitated by introducing two scalar fields which satisfy a mixed boundary condition on one surface of the wedge and a Neumann or Dirchlet boundary condition on the other. A functional transformation is employed to simplify the boundary conditions so that eigenfunction expansions can be obtained for the resulting Green's functions. The eigenfunction expansions are transformed into the integral representations which then are evaluated asymptotically by the modified Pauli-Clemmow method of steepest descent. A far zone approximation is made to obtain the scattered field from which the diffraction coefficient is found for scalar plane, cylindrical or sperical waves incident on the edge. With the introduction of a ray-fixed coordinate system, the dyadic diffraction coefficient for plane or cylindrical EM waves normally incident on the edge is reduced to the sum of two dyads which can be written alternatively as a 2 X 2 diagonal matrix. This format is consistent with that being used in other Geometrical Theory of Diffraction studies being conducted at the Electro-Science Laboratory. The dyadic diffraction coefficient is valid in the transition region of the shadow and reflection boundaries. It is composed of trigonometric functions and Fresnal integrals which are easy to compute.

17. Key Words (Suggested by Author(s))	18. Distribution Statement
Antennas, Spacecraft and Aircraft Antennas Applied Electromagnetic Theory	Unclassified - Unlimited STAR Category 09

19. Security Classif. (of this report)	20. Security Classif. (of this page)	21. No. of Pages	22. Price*
Unclassified	Unclassified	91	$4.00

*For sale by the National Technical Information Service, Springfield, Virginia 22151

TABLE OF CONTENTS

		Page
I.	INTRODUCTION	1
II.	SCALAR WAVE DIFFRACTION	7
	A. Cylindrical Wave Illumination	8
	B. Plane Wave Illumination	22
	C. Spherical Wave Illumination	23
III.	ELECTROMAGNETIC WAVE DIFFRACTION	27
	A. Cylindrical Wave Illumination	29
	B. Plane Wave Illumination	36
IV.	APPLICATIONS AND NUMERICAL RESULTS	40
V.	DISCUSSIONS	58
Appendix		
	I. AN ASYMPTOTIC APPROXIMATION FOR SCALAR WEDGE DIFFRACTION VIA THE MODIFIED STEEPEST DESCENT METHOD	68
	A. Cylindrical Wave Illumination	68
	B. Plane Wave Illumination	79
	C. Spherical Wave Illumination	81
REFERENCES		87

Page Intentionally Left Blank

CHAPTER I
INTRODUCTION

The diffraction by a right-angled wedge is an important geometry in the analysis of many radiating systems. Although the diffraction of electromagnetic waves by a perfectly-conducting wedge has been studied extensively, few results exist for the case where one surface of the right-angled wedge is covered by a dielectric slab, an absorber coating, slightly rough or is corrugated. Such wedge configurations are of importance to problems of technology not only because they occur in practical structures but also because of design considerations where there is a need for the modification or control of edge diffraction. It is extremely difficult to find an exact solution to the diffraction by a wedge with coated or corrugated surfaces; however the problem becomes tractable if the boundary condition at this surface can be approximated by a surface impedance.

A one-side dielectric loaded right-angled wedge is depicted in Fig. 1. If the dielectric slab is thin enough and the radiation from the end face of the slab at the edge of the wedge can be neglected, the dielectric-covered ground plane can be approximated as a reactive surface. This approximate electromagnetic boundary condition depends on the polarization of incident wave. For the TE case, the surface admittance, y_s, is given as

$$y_s = - j \frac{(\xi d) \cot(\xi d)}{z_0 (kd)} \quad ,$$

where ξd is obtained from the solution of the transcendental equation

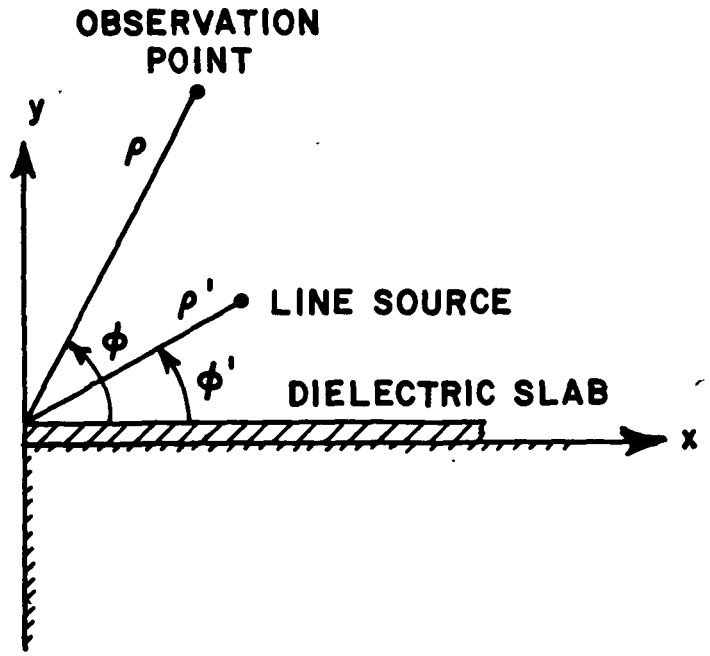

Fig. 1. The 2-D conducting right-angled wedge with one side covered by a dielectric slab and a line source in the cylindrical coordinate system.

$$(\xi d)\cot(\xi d) + \sqrt{(\varepsilon_r - 1)(kd)^2 - (\xi d)^2} = 0;$$

whereas for the TM case, the surface impedance

$$z_s = j \frac{z_o}{(kd)} \times \frac{(\xi d)}{\varepsilon_r} \tan(\xi d),$$

where (ξd) is determined from another transcendental equation

$$(\xi d)\tan(\xi d) - \sqrt{(\varepsilon_r - 1)(kd)^2 - (\xi d)^2} = 0.$$

k and z_o are the wave number and characteristic impedance of free space, and d and ε_r are the thickness and the relative permittivity of dielectric cover. Admittedly the surface impedance is an approximate boundary condition of limited validity, but its use may be adequate to approximate the important characteristics of the scattered

field; moreover, in principle it can be extended and improved[11]. Other physical configurations which can be approximated by this impedance model are a conducting surface coated with an absorbing material, a special case of a rough surface[23] and a corrugated perfectly conducting surface with rectangular grooves, providing the groove spacing is small compared to the wavelength.

The problem considered in this report is the diffraction of plane and cylindrical electromagnetic waves normally incident on the edge of a right-angled wedge; where one surface of the wedge is represented by a uniform finite surface impedance and the other is perfectly conducting or has a surface impedance of zero. The diffraction of an obliquely incident scalar spherical wave is also treated. The solution is formulated in terms of two scalar fields which satisfy a uniform impedance boundary condition at one surface of the wedge and a Neumann or Dirichlet condition at the other.

The difficulty of this mixed boundary condition can be overcome by a simple functional transformation. The transformation is made in such a way that the mixed boundary condition becomes a simple homogeneous one. The Green's function resulting from the transformation can thus be found in the usual way. The final solution is obtained by an inverse transformation. This idea was first given by Lewy[15] and Stoker[24] who studied problems in water wave theory. The same idea has been applied by Karp and Karal[7,9], Chu[1], Karal et al[8] and Chu et al[2] for solving electromagnetic diffraction problems for a right-angled wedge; one of its surfaces sustains a surface wave, while the other is a perfectly conducting surface. The wedge is illuminated by a normally incident plane wave, a magnetic line source on the vertex or an incident surface wave. In all the above cases, the solution is obtained by requiring that after the inverse transformation, the derivative of the total field and the field itself must be continuous across the positive y-axis: $x=0$, $y>0$ (see Fig. 2). The

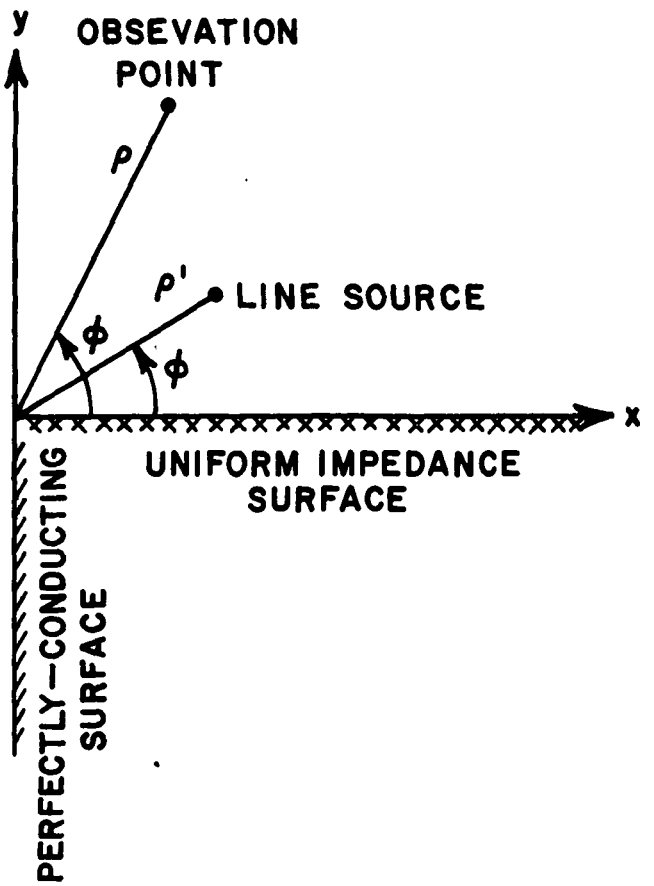

Fig. 2. The surface impedance model of a 2-D right-angled wedge with one wedge surface covered by a dielectric slab.

solution is given in the far zone. In the case of a normally incident plane wave illumination, the diffracted field becomes singular at the reflection and shadow boundaries. Karp[10] also obtained a two dimensional Green's function for a right-angled wedge under an impedance boundary condition which does not support surface waves. One of the constants in his solution is, in general, difficult to compute. Using a different method we have obtained a simple expression for this constant.

In this report the transformation technique is extended to solve the diffraction of spherical waves. Also the relationship of the scalar solutions to the EM problem are considered. The transformed solutions consist of some special Green's functions which satisfy Neumann or Dirichlet boundary conditions at the surfaces of the wedge. Integral representations are obtained from the eigenfunction expansions of these Green's functions. The integrals are then evaluated asymptotically via the modified Pauli-Clemmow method of steepest descent[20] to obtain a far-zone approximation. The solutions are given in terms of a geometrical optics field and a diffracted field. The geometrical optics field consists of the incident field and the reflected field which comes from pole contributions to the integral. Saddle point contributions from the integral yield the diffracted field. A diffraction coefficient is obtained which is also valid in the transition region of the shadow and reflection boundaries. The geometrical optics field is discontinuous across the shadow and reflection boundaries; however the total field, which is the sum of the geometrical optics field and the diffracted field, is continuous.

The scalar diffraction coefficients are derived in Chapter II. The wedge illuminated by a line source is treated first. By letting the line source recede to infinity, the diffraction coefficients for plane wave illumination are obtained. The problem for a point source illumination of the wedge can be related to that of a line source illumination by a Fourier transformation on the z (edge-directed)-coordinate. The scalar diffraction coefficients are composed of trigonometric functions and Fresnel integrels which are easy to compute.

In Chapter III, the diffraction of normally incident electromagnetic waves is treated. A ray-fixed coordinate system is introduced to represent the diffracted electromagnetic field. When the components

of the incident and diffracted fields are expressed in this coordinate system, and the only leading term in the asymptotic solution is retained, the resulting expression for the dyadic diffraction coefficient reduces to a sum of two dyads; in the matrix notation, this diffraction coefficient is a 2x2 diagonal matrix.

It is shown in Chapter IV that the solution derived in the preceding chapters can be reduced to that of a perfectly-conducting wedge[20] and that it can be applied to a right-angled wedge with an impedance boundary condition illuminated by a magnetic line source at its vertex[9]. The radiation from a magnetic line source located close to the reactive surface of a right-angled wedge and the radiation from slots in truncated, dielectric-covered surfaces are considered. In both cases, the calculated and measured patterns are in good agreement. Patterns are given for different impedance-loaded wedges illuminated by a magnetic (or electric) current line source at different locations, and some observations are made concerning the behavior of the scattered field.

We conclude this chapter by briefly describing the related work of Felson[3], Malyughinetz[17,18] and Mohsen and Hamid[19]. Felson has solved the scalar wedge diffraction problem for an arbitrary-angled wedge when the surface impedance is proportional to the radial variable ρ. Because of this special boundary condition, the problem is separable and a Green's function can be obtained by standard methods. The uniform impedance boundary condition in our problem makes it impossible to apply the separation of variables method directly in this way.

Malyughinetz considered the scalar diffraction by an arbitrary-angled wedge with different impedance boundary conditions on its two surfaces; he restricted his solution to plane wave illumination. The solution is obtained by a method analogous to the one used by

Peters[21] and Senior[22]. With this method the differential equation and boundary conditions are expressed as a difference equation for the determination of a regular function whose real part represents the velocity potential. The exact solution thus obtained can be applied to our problem for the plane wave illumination if one of the surface impedances vanishes; however the integrals in his solution are difficult to compute because they are improper with meromorphic functions as their integrands. At shadow and reflection boundaries, his solution appears to be singular.

Mohsen and Hamid have made a different approximation in their approach to the diffraction of electromagnetic waves by a perfectly-conducting arbitrary-angled wedge covered by a thin dielectric slab on one surface. They treat the diffraction of an E-polarized plane wave normally incident on the edge. It is assumed that the dielectric slab is thin with the relative permittivity not much larger than unity and that the slab is in the illuminated region. By imposing an approximate boundary condition, $E^s \sim \Gamma E^i$, which is valid only in the far zone, at the dielectric covered surface, where Γ is the plane wave reflection coefficient for a dielectric slab on an infinite ground plane, the solution is obtained in an integral form, which is then evaluated asymptotically in terms of Fresnel integrals.

CHAPTER II
SCALAR WAVE DIFFRACTION

In this chapter the diffraction by a right-angled wedge is formulated mathematically as a boundary value problem. One side of the wedge surface satisfies a uniform impedance boundary condition; the other a Dirichlet or Neumann boundary condition. Plane wave, cylindrical wave and spherical wave illuminations of the edge are considered separately.

A. Cylindrical Wave Illumination

Consider a z-directed, uniform line source of unit strength radiating in the presence of a right-angled wedge with its edge also oriented in the z-direction (see Fig. 2). The total field $U_{\substack{a\\b}}$, which consists of the incident and scattered components, satisfies the scalar wave equation

$$(1) \qquad (\nabla_t^2 + k^2)\, U_{\substack{a\\b}} = -\,\delta(x-x')\,\delta(y-y')$$

with boundary conditions

$$(2) \qquad \frac{\partial U_{\substack{a\\b}}}{\partial y} + \lambda_{\substack{a\\b}} U_{\substack{a\\b}} = 0 \quad ; \quad \phi = 0$$

$$(3a) \qquad U_a = 0 \quad ; \quad \phi = \frac{3\pi}{2}$$

or

$$(3b) \qquad \frac{\partial U_b}{\partial \phi} = 0 \quad ; \quad \phi = \frac{3\pi}{2}$$

$$(4) \qquad \lim_{\pi\to\infty} \sqrt{\rho}\,(U_{\rho,\substack{a\\b}} + j\,k\,U_{\substack{a\\b}}) \longrightarrow 0 \quad , \quad 0 < \phi < \frac{3\pi}{2}$$

and

$$(5) \qquad U_{\substack{a\\b}} \text{ is finite except at the point } (x',y').$$

Here ∇_t^2 is the two dimensional Laplician operator, $\delta(x-x')$ is the Dirac Delta function, k is the wave number of the linear, homogeneous, isotropic medium surrounding the wedge. Condition (2) is a surface

impedance boundary condition; the subscripts a and b are used to denote the different surface impedances required in the EM problem to follow. In an acoustic problem, the surface impedance expresses a ratio of pressure to velocity; in an electromagnetic problem, it is a ratio of the tangential component of the electric field to the tangential component of the magnetic field. An impedance boundary surface may arise from an absorbing coating or thin dielectric slab on the surface or corrugations in the surface. Condition (3a) represents a soft boundary for the acoustic case whereas (3b) represents a hard boundary for the acoustic case; mathematically these are the homogeneous Dirichlet and Neumann boundary conditions, respectively. Condition (4) represents the Sommerfeld radiation condition and (5) represents the Meixner edge condition. A time dependence, $e^{j\omega t}$, is assumed and suppressed.

Let us make a functional transformation

$$V = \left(\frac{\partial}{\partial y} + \lambda\right) U. \tag{6}$$

For simplicity, let U represent either U_a or U_b. By using the fact that the operators $(\nabla_t^2 + k^2)$ and $\left(\frac{\partial}{\partial y} + \lambda\right)$ commute and $\frac{\partial}{\partial y}\,\delta(y-y') = -\frac{\partial}{\partial y'}\,\delta(y-y')$, V must be such that

$$(\nabla_t^2 + k^2)\, V = \left(\frac{\partial}{\partial y'} - \lambda\right) \delta(x-x')\, \delta(y-y') \tag{7}$$

and also satisfies the boundary conditions

$$V = 0 \quad ; \quad \phi = 0 \tag{8a}$$

and

(8b) $$\begin{matrix} V_a = 0 \\ \frac{\partial V_b}{\partial x} = 0 \end{matrix} \quad ; \quad \phi = \frac{3\pi}{2}$$

and the Sommerfeld radiation condition. It is worthwhile to mention that this transformation technique cannot generally be applied to an arbitrary-angled wedge since the boundary condition of V at the other wedge surface does not become simple except for some special angular space which, in this case, is a right-angled wedge. The function V need not be finite at the origin because it involves a differentiation of U. Let us consider a Green's function G which satisfies the conditions

(9) $$(\nabla_t^2 + k^2)G = -\delta(x-x')\,\delta(y-y') \quad , \quad 0 < \phi < \frac{3\pi}{2}$$

(10) $$G = 0 \quad , \quad \phi = 0$$

and conditions (3), (4) and (5) for the wedge. It can be shown that

(11a) $$G = -\frac{j}{6} \sum_{m=0}^{\infty} \varepsilon_m J_{\frac{2m}{3}}(k\rho_<) H^{(2)}_{\frac{2m}{3}}(k\rho_>) \left[\cos\frac{2m}{3}(\phi-\phi') - \cos\frac{2m}{3}(\phi+\phi')\right], \quad \text{for (3a)}$$

and

(11b) $$G = -\frac{j}{3} \sum_{m=0}^{\infty} J_{\frac{2m+1}{3}}(k\rho_<) H^{(2)}_{\frac{2m+1}{3}}(k\rho_>) \left[\cos\frac{2m+1}{3}(\phi-\phi') - \cos\frac{2m+1}{3}(\phi+\phi')\right], \quad \text{for (3b)},$$

where

$$0 \leq \phi, \phi' \leq \frac{3\pi}{2}$$

$$0 \leq \rho, \rho' < \infty \quad ,$$

and

$$\varepsilon_m = 1, \qquad m = 0$$
$$= 2, \qquad m \neq 0.$$

$J_{\nu m}(k\rho)$ and $H^{(2)}_{\nu m}(k\rho)$ represent the cylindrical Bessel function of the first kind and the cylindrical Hankel function of the second kind, respectively, and

$$\rho_< = \begin{cases} \rho & \text{when} \quad \rho < \rho' \\ \rho' & \qquad\quad \rho > \rho' \end{cases}$$

$$\rho_> = \begin{cases} \rho & \text{when} \quad \rho > \rho' \\ \rho' & \qquad\quad \rho < \rho' \end{cases}$$

Applying the operator $-\left(\frac{\partial}{\partial y'} - \lambda\right)$ to G, we obtain a unique function $\psi = -\left(\frac{\partial}{\partial y'} - \lambda\right)G$, which satisfies not only the conditions imposed in U, but also condition (5). This function ψ is a particular solution of U. The complete solution to U is the sum of the particular solution and the homogeneous solution. By using separation of variables and applying the radiation condition, it can be shown that the homogeneous solution is of the form

$$(12) \qquad \sum_{m=0}^{\infty} H^{(2)}_{\nu m}(k\rho)\,[\alpha_m \cos\nu_m\phi + \beta_m \sin\nu_m\phi].$$

This homogeneous solution is singular. Since U must be finite, V cannot be too singular. Hence, of all the terms in Eq. (12), only

those terms for which $\nu_m < 1$ are retained in the construction of V. Note $\alpha_m = 0$ and $\nu_m = \frac{2}{3}m$ if Eq. (3a) holds, while $\beta_m = 0$ and $\nu_m = \frac{2m+1}{3}$ if Eq. (3b) holds. Thus V contains some parameters which are to be determined.

We shall now introduce another approach to obtain the homogeneous solution for V[10]. Consider the Green's function W, satisfying the conditions (1), (3), (4) and (5), and the boundary condition

$$\frac{\partial W}{\partial y} = 0 , \qquad \phi = 0. \tag{13}$$

It can be shown that W can be given by a convergent eigenfunction expansion as

$$W = -\frac{j}{6} \sum_{m=0}^{\infty} J_{\frac{2m+1}{3}}(k\rho_<)\, H^{(2)}_{\frac{2m+1}{3}}(k\rho_>) \left[\cos\frac{2m+1}{3}(\phi-\phi') + \cos\frac{2m+1}{3}(\phi+\phi')\right] \qquad \text{for (3a).} \tag{14a}$$

and

$$W = -\frac{j}{3} \sum_{m=0}^{\infty} \varepsilon_m J_{\frac{2m}{3}}(k\rho_<)\, H^{(2)}_{\frac{2m}{3}}(k\rho_>) \left[\cos\frac{2m}{3}(\phi-\phi') + \cos\frac{2m}{3}(\phi+\phi')\right] \qquad \text{for (3b).} \tag{14b}$$

From Eq. (1) we can prove that

$$(\nabla_t^2 + k^2)\left[\frac{\partial G}{\partial y'} + \frac{\partial W}{\partial y}\right] = -\left(\frac{\partial}{\partial y'} + \frac{\partial}{\partial y}\right)\delta(x-x')\,\delta(y-y') \equiv 0. \tag{15}$$

Hence the function $H \equiv \frac{\partial G}{\partial y'} + \frac{\partial W}{\partial y}$ is a solution of the homogeneous wave equation. Furthermore, this function, H, obeys conditions (3a) (or (3b)) and (4), vanishes at $\phi = 0$, satisfies the radiation condition and

behaves at the origin like the non-vanishing terms in the series Eq. (12) which was used to represent the singular solution to be added to ψ. Therefore, we obtain a complete solution for V as

$$V = -\left(\frac{\partial}{\partial y'} - \lambda\right) G + C\left(\frac{\partial G}{\partial y'} + \frac{\partial W}{\partial y}\right), \tag{16}$$

where C is a constant to be determined.

Once V is found, we can obtain the solution for the problem involving U since Eq. (6) can be integrated. A particular solution of Eq. (6) is

$$U_p = e^{-\lambda y} \int_{-\infty}^{y} e^{\lambda \xi} V(x,\xi) d\xi , \qquad \text{Re } \lambda > 0 \tag{17a}$$

$$U_p = - e^{-\lambda y} \int_{y}^{\infty} e^{\lambda \xi} V(x,\xi) d\xi, \qquad \text{Re } \lambda < 0. \tag{17b}$$

It should be noted that the above integrals are convergent and hence exist. In the far zone, we observe that U, V, G and W have the asymptotic formulas

$$G \to \frac{e^{-jk\rho}}{\sqrt{\rho}} g(\phi;x',y') \tag{18a}$$

$$W \to \frac{e^{-jk\rho}}{\sqrt{\rho}} w(\phi;x',y') \tag{18b}$$

$$V \to \frac{e^{-jk\rho}}{\sqrt{\rho}} v(\phi;x',y') \tag{18c}$$

and

$$U \to \frac{e^{-jk\rho}}{\sqrt{\rho}} U(\phi;x',y'). \tag{18d}$$

Here G, V and W are known functions and U is to be found. Since the far-zone field is of interest, only those terms which are of $O(\frac{1}{\sqrt{\rho}})$ are retained, the operator $\frac{\partial}{\partial y}$ can be approximated then by $-j\,k\,\sin\phi$; thus we obtain

$$(19) \qquad (-j\,k\,\sin\phi + \lambda)U \simeq V,$$

which can also be written as

$$(20) \qquad U \simeq (C-1)\,\frac{\frac{\partial G}{\partial y'} - jk\sin\phi W}{\lambda - jk\sin\phi} + \frac{\lambda G - jk\sin\phi W}{\lambda - jk\sin\phi} \quad .$$

In Appendix I, G and W are transformed into the integral representations and then computed asymptotically for the large parameter $\frac{k\rho\rho'}{\rho+\rho'}$. From the asymptotic solution, we can identify the ray-optical behavior of the field. The incident field is

$$U^i = -\frac{j}{4}\sqrt{\frac{2j}{\pi k(\rho^2+\rho'^2-2\rho\rho'\cos(\phi-\phi'))^{1/2}}}\ x$$

$$x\ e^{-jk\sqrt{\rho^2+\rho'^2-2\rho\rho'\cos(\phi-\phi')}}\ H(\pi-|\phi-\phi'|),$$

where H(t) is the Heaviside unit function defined as

$$(21) \qquad H(t) = \begin{cases} 0 & , \quad t < 0 \\ 1 & , \quad t > 0 \end{cases} \quad .$$

From this we obtain

$$(22) \qquad C = 1.$$

Thus Eq. (20) becomes

$$(23) \qquad U \sim \frac{\lambda G - jk\sin\phi W}{\lambda - jk\sin\phi} \quad .$$

The reflected field from the surface at $\phi = 0$ is given by

$$(24) \qquad U^r = R \times \left(- \frac{j}{4} \sqrt{\frac{2j}{\pi k (\rho^2+\rho'^2-2\rho\rho'\cos(\phi+\phi'))^{1/2}}} \right) \times e^{-jk\sqrt{\rho^2+\rho'^2-2\rho\rho'\cos(\phi+\phi')}} H(\pi-|\phi+\phi'|),$$

where R is the reflection coefficient for an impedance surface, which is given as

$$(25) \qquad R = \frac{jk\sin\phi+\lambda}{jk\sin\phi-\lambda} \quad .$$

The reflected field due to the perfectly-conducting surface $\phi = \frac{3\pi}{2}$ is

$$(26) \qquad U^r = \begin{pmatrix} -1 \\ 1 \end{pmatrix} \times \left(- \frac{j}{4} \sqrt{\frac{2j}{\pi k (\rho^2+\rho'^2-2\rho\rho'\cos(\pi-(\phi+\phi'))^{1/2}}} \right) \times e^{-jk\sqrt{\rho^2+\rho'^2-2\rho\rho'\cos(\pi-(\phi+\phi')}} H(\pi-|3\pi-(\phi+\phi')|)$$

where "-1" and "1" are the reflection coefficients corresponding to the boundary conditions (3a) and (3b), respectively. The incident and reflected field components are found from the pole contributions enclosed in the appropriate closed path which is given in Appendix I. The saddle point contribution yields the diffracted ray field. Therefore, in accordance with the geometrical theory of diffraction, U^d can be written as

$$(27) \qquad \begin{matrix} U^d_a \\ b \end{matrix} \sim U^i \begin{matrix} D_a \\ b \end{matrix} \frac{e^{-jk\rho}}{\sqrt{\rho}}$$

in which

$$U^i \sim -\frac{j}{4}\frac{2j}{\pi k\rho'}e^{-jk\rho'} \quad .$$

D_a is the diffraction coefficient for the boundary condition (3a) and D_b is the diffraction coefficient for condition (3b), which are given as

$$D_a = \frac{\lambda_a D_s - jk\sin\phi\, D_{g1}}{\lambda_a - jk\sin\phi} \tag{28}$$

where

$$D_{g1} = -\frac{e^{-j\frac{\pi}{4}}}{3\sqrt{2\pi k}}\left\{2\sin\frac{\pi}{3}\left[\cos\frac{\beta^-}{3} + \cos\frac{\beta^+}{3}\right]\right\} + \tag{29a}$$

$$+ d_g^+(\beta^-)F[\kappa a^+(\beta^-)] + d_g^-(\beta^-)F[\kappa a^-(\beta^-)] +$$

$$+ d_g^+(\beta^+)F[\kappa a^+(\beta^+)] + d_g^-(\beta^+)F[\kappa a^-(\beta^+)]$$

$$d_g^{\pm}(\beta) = \frac{\cos^2\frac{\pi\pm\beta}{3}}{\sin\frac{\pi\pm\beta}{3}} \tag{29b}$$

$$D_s = \left[d^+(\beta^-)F[\kappa a^+(\beta^-)] + d^-(\beta^-)F[\kappa a^-(\beta^-)]\right] \tag{29c}$$

$$- \left[d^+(\beta^+)F[\kappa a^+(\beta^+)] + d^-(\beta^+)F[\kappa a^-(\beta^+)]\right]$$

$$d^{\pm}(\beta) = -\frac{e^{-j\frac{\pi}{4}}}{3\sqrt{2\pi k}}\cot\frac{\pi\pm\beta}{3} \quad , \tag{29d}$$

and

$$D_b = \frac{\lambda_b D_{g2} - jk\sin\phi\, D_h}{\lambda_b - jk\sin\phi} \tag{30}$$

where

$$(31a)\qquad D_{g2} = -\frac{e^{-j\frac{\pi}{4}}}{3\sqrt{2\pi k}}\left\{2\sin\frac{\pi}{3}\left[\cos\frac{\beta^-}{3} - \cos\frac{\beta^+}{3}\right] + \right.$$

$$\left. + \; d_g^+(\beta^-)F[\kappa a^+(\beta^-)] + d_g^-(\beta^-)F[\kappa a^-(\beta^-)]\right\} -$$

$$- \; d_g^+(\beta^+)F[\kappa a^+(\beta^+)] + d_g^-(\beta^+)F[\kappa a^-(\beta^+)]$$

$$(31b)\qquad D_h = \left[d^+(\beta^-)F[\kappa a^+(\beta^-)] + d^-(\beta^-)F[\kappa a^-(\beta^-)]\right] +$$

$$+ \left[d^+(\beta^+)F[\kappa a^+(\beta^+)] + d^-(\beta^+)F[\kappa a^-(\beta^+)]\right] \quad .$$

and

$$\beta = \beta^{\pm} \equiv \phi \pm \phi', \quad \kappa = \frac{k\rho\rho'}{\rho+\rho'} \quad .$$

$$(32)\qquad F[\kappa a^{\pm}(\beta)] = 2j\,\kappa a^{\pm}(\beta)\, e^{j\kappa a^{\pm}(\beta)} \int_{\sqrt{\kappa a^{\pm}(\beta)}}^{\infty} e^{-jt^2}\, dt,$$

where the positive branch of the square root is taken, and

$$a^{\pm}(\beta) = 1 + \cos(-\beta + 3\,N^{\pm}\pi).$$

The value of $N^{\pm}$ is determined by the integer which most closely satisfies the equation:

$$3\,N^{\pm}\pi - \beta = \pm\,\pi.$$

Outside the transition regions of shadow and reflection boundaries, $(\kappa a^{\pm}(\beta) >> 1$. $F[\kappa a^{\pm}(\beta)]$ in Eq. (32) tends to 1. D_{s} and D_{g1} D_{h} D_{g2} can be simplified as

$$(33)\qquad D_{s,h} = \frac{2e^{-j\frac{\pi}{4}}\sin\frac{2\pi}{3}}{3\sqrt{2\pi k}}\left[\frac{1}{\cos\frac{2\pi}{3} - \cos\frac{2}{3}(\phi-\phi')} \mp \frac{1}{\cos\frac{2\pi}{3} - \cos\frac{2}{3}(\phi-\phi')}\right]$$

and

$$(34)\qquad D_{g1,g2} = \frac{4e^{-j\frac{\pi}{4}}\sin\frac{\pi}{3}}{3\sqrt{2\pi k}}\left[\frac{\cos(\frac{\phi-\phi'}{3})}{\cos\frac{2\pi}{3} - \cos\frac{2}{3}(\phi-\phi')} \pm \frac{\cos(\frac{\phi+\phi'}{3})}{\cos\frac{2\pi}{3} - \cos\frac{2}{3}(\phi+\phi')}\right];$$

which become singular when $\frac{2}{3}(\phi\pm\phi') = \frac{2\pi}{3} + 2N\pi$, i.e., at the shadow and reflection boundaries.

Thus, the region surrounding the wedge can be divided into three regions by the reflection boundary $\phi = \pi - \phi'$ and shadow boundary $\phi = \pi + \phi'$, such as shown in Fig. 3.* The total field is given by

$$(35)\qquad U \sim \begin{cases} U^i + U^r + U^d, & 0 \le \phi < \pi - \phi' \\ U^i + U^d, & \pi - \phi' < \phi < \pi + \phi' \\ U^d, & \pi + \phi' < \phi \le \frac{3\pi}{2}. \end{cases}$$

When the line source is near the impedance surface and far from the edge of the wedge, the surface wave is excited if the impedance surface supports a surface wave. The strength of excitation of the surface wave is assumed to be the same as those due to a uniform line source located above an impedance surface of infinite extent. Let U_s be the excited surface field. It can be shown that

*We have chosen the example where only the surface $\phi=0$ is illuminated; the discussion for the two other possible cases follows in an analogous way.

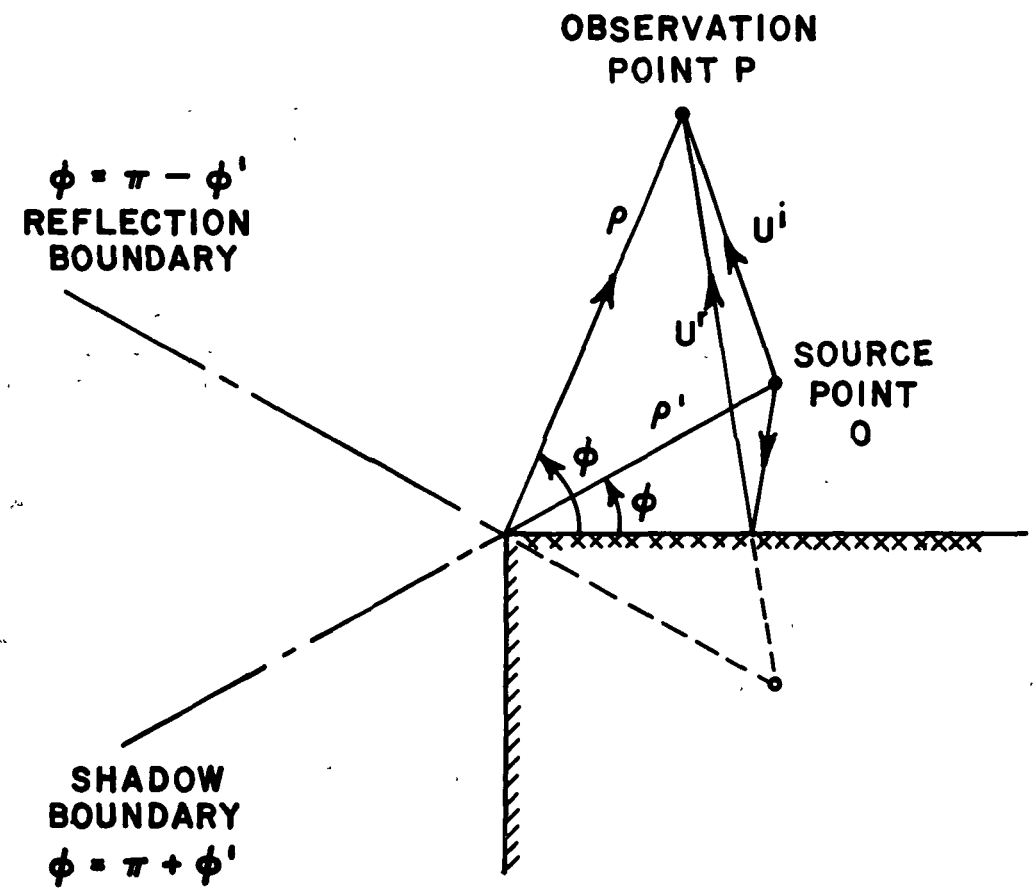

Fig. 3. The reflection boundary and shadow boundary of a line source illuminating on a 2-D right-angled wedge.

$$(36) \qquad U_s = -j\frac{\lambda}{\beta} e^{-\lambda(y+y')} e^{-j\beta x}, \qquad x > 0$$

where $\beta = \sqrt{k^2+\lambda^2}$ is the wave number of the surface wave. This excited surface wave propagates along the impedance surface $\phi=0$ and does not radiate until the impedance surface is terminated by the edge of the wedge. The source is assumed to be sufficiently removed from the edge so that the infinite surface representation is valid. Chu[1,2] studied the radiation field of the surface wave diffraction by a right-angled wedge in which TE and TM surface wave diffraction were considered. TE surface wave diffraction corresponds to our

problem with the boundary condition (3a); TM surface wave diffraction, the boundary condition (3b). The TE surface wave diffracted field, U^d_{sa}, was given[1] as

$$U^d_{sa} = U_s\, D_{sa}\, \frac{e^{-jk\rho}}{\sqrt{\rho}} \tag{37a}$$

whereas the TM surface wave diffracted field

$$U^d_{sb} = U_s\, D_{sb}\, \frac{e^{-jk\rho}}{\sqrt{\rho}} \tag{37b}$$

where

$$D_{sa} = B_1 \sqrt{\frac{2}{\pi k}}\, \frac{\sin\frac{2\phi}{3}}{jk\sin\phi - \lambda}\, e^{j\frac{7\pi}{12}} \tag{38a}$$

and

$$D_{sb} = A_o \sqrt{\frac{2}{\pi k}}\, \frac{\sin\frac{\phi}{3}}{jk\sin\phi - \lambda}\, e^{j\frac{5\pi}{12}} \tag{38b}$$

A_o and B_1 are constants and are given by

$$A_o = \frac{-4j\sqrt{k^2+\lambda^2}}{3j\sqrt{k^2+\lambda^2}\, I_{\frac{1}{3}} + \sqrt{3}\left(I_{\frac{1}{3}}\lambda - I_{\frac{2}{3}} k\, e^{-j\frac{2\pi}{3}}\right)} \tag{39}$$

and

$$B_1 = \frac{-4j\sqrt{k^2+\lambda^2}}{j\sqrt{3}\sqrt{k^2+\lambda^2}\, I_{\frac{2}{3}} + 3\left(\lambda I_{\frac{2}{3}} - k\, e^{-j\frac{\pi}{3}} I_{\frac{1}{3}}\right)} \tag{40}$$

I_ν is the Laplace transformation of $H_\nu^{(2)}(k|\xi|)$ and

$$(41) \qquad I_\nu = \frac{\left(\sqrt{k^2+\lambda^2}-\lambda\right)^\nu}{k\sqrt{k^2+\lambda^2}} \left\{1 - \frac{j}{\sin\nu\pi}\left[\cos\nu\pi - \frac{\left(\lambda+\sqrt{k^2+\lambda^2}\right)^{2\nu}}{k^2}\right]\right\} ,$$

where $-1 < \mathrm{Re}\nu < 1$.

In summary, the solution is obtained asymptotically in the far zone. When the impedance surface does not support a surface wave, the total field is given by Eq. (35). If the impedance surface sustains a surface wave and the line source is located close to the impedance surface and far from the edge, the diffracted field due to the surface wave excited by the line source must be taken into account. Note that the strength of excitation of the surface wave is proportional to $e^{-\lambda y'}$. Thus the excited surface wave has an important effect only when y' is small ($\phi' << \frac{\pi}{2}$). The total radiation field is then given by

$$(42) \qquad U \sim \begin{cases} U^i + U^r + U^d + U_s^d & , \quad 0 \le \phi < \pi - \phi' \\ U^i + U^d + U_s^d & , \pi - \phi' < \phi < \pi + \phi' \\ U^d + U_s^d & , \pi + \phi' < \phi \le \frac{3\pi}{2} \end{cases} .$$

Note that there is also a surface wave, $C_2\, e^{-\lambda y + j\beta x}$, propagating away from the edge due to the termination of the edge of the wedge. The strength of this surface wave, C_2, can be determined by another method which will be mentioned in Chapter V. This surface wave field is significant only when y is small ($\phi \simeq 0$) and it does not radiate unless the impedance surface is truncated. The total field is the sum of U given by Eq. (42) and $C_2\, e^{-\lambda y + j\beta x}$ which exists only in the region $\{x>0,\ y>0\}$.

The diffracted field, U_s^d, due to the excited surface wave is continuous in the whole region. The diffracted field, U^d, yields a uniformly asymptotic representation for the total field so that it properly compensates for the discontinuity in the geometrical optics fields, the incident field U^i and the reflected field U^r, across the transition boundaries, thereby, yielding a total field which is continuous everywhere.

B. Plane Wave Illumination

The plane wave incidence case can be treated as a special case of the cylindrical wave illumination. By letting $\rho' \to \infty$ in the line source case of Section A and factoring out the "line source factor"

$$-\frac{j}{4}\sqrt{\frac{2j}{\pi k\rho'}}\,e^{-jk\rho'},$$

the result for the plane wave case can thus be obtained. The details of the derivation are given in the Appendix I. Note that the total field, $U_{\substack{a\\b}}^p$, due to a plane wave normally incident on the edge of the wedge satisfies the 2-dimensional, homogeneous scalar Helmholtz equation

$$(\nabla_t^2 + k^2)\, U_{\substack{a\\b}}^p (\rho,\phi;\phi') = 0, \tag{43}$$

where the subscript a (or b) indicates that the total field satisfies boundary condition (3a) (or (3b)), in addition to (2), (4) and (5).

For a plane wave of unit amplitude and with its phase reference located at the edge, the diffracted field is given by

$$U_{\substack{a\\b}}^d \sim D_{\substack{a\\b}} \frac{e^{-jk\rho}}{\sqrt{\rho}} \tag{44}$$

where D_a is given in Eq. (28) or Eq. (30). In the diffraction coefficients, the large parameter $\frac{k\rho\rho'}{\rho+\rho'} = k\rho$ since $\rho' \to \infty$.

C. Spherical Wave Illumination

Consider the case of a scalar point source illumination of the wedge. The point source generates scalar, spherical waves. Let the point source be located at $\bar{s}'(\rho',\phi',z')$ as shown in Fig. 4. For a source of unit strength, the total field $U_{\substack{a\\b}}(\rho,\phi,z;\rho',\phi',z')$ due to spherical waves incident on the wedge satisfies

$$(45) \qquad (\nabla^2 + k^2)U_{\substack{a\\b}}(\bar{s},\bar{s}') = -\delta(x-x')\delta(y-y')\delta(z-z'),$$

and conditions (2), (4) and (5) as before, U_a satisfies the additional boundary condition (3a), whereas U_b satisfies (3b). Note that $\nabla^2 = \nabla_t^2 + \frac{\partial^2}{\partial z^2}$ is the 3-dimensional Laplician operator. Because of the special geometry of the wedge, this 3-dimensional problem can be reduced to a 2-dimensional problem via a Fourier integral transformation. Let

$$(46) \qquad \tilde{U}_{\substack{a\\b}}(\rho,\phi,h;\rho',\phi',z') = \int_{-\infty}^{\infty} U_{\substack{a\\b}}(\bar{s},\bar{s}')\, e^{-jhz}dz$$

$$(47) \qquad U_{\substack{a\\b}}(\bar{s},\bar{s}') = \frac{1}{2\pi}\int_{-\infty}^{\infty} \tilde{U}_{\substack{a\\b}}(\rho,\phi,h;\rho',\phi',z')\, e^{jhz}dh.$$

Equations (46) and (47) form a Fourier transform pair. Let us assume the existence of the transform pair; then the Fourier transform of Eq. (45) yields

$$(48) \qquad (\nabla_t^2+k_t^2)\,\tilde{U}_{\substack{a\\b}}(\rho,\phi,h;\rho',\phi',z') = -\delta(x-x')\delta(y-y')\, e^{-jhz'}$$

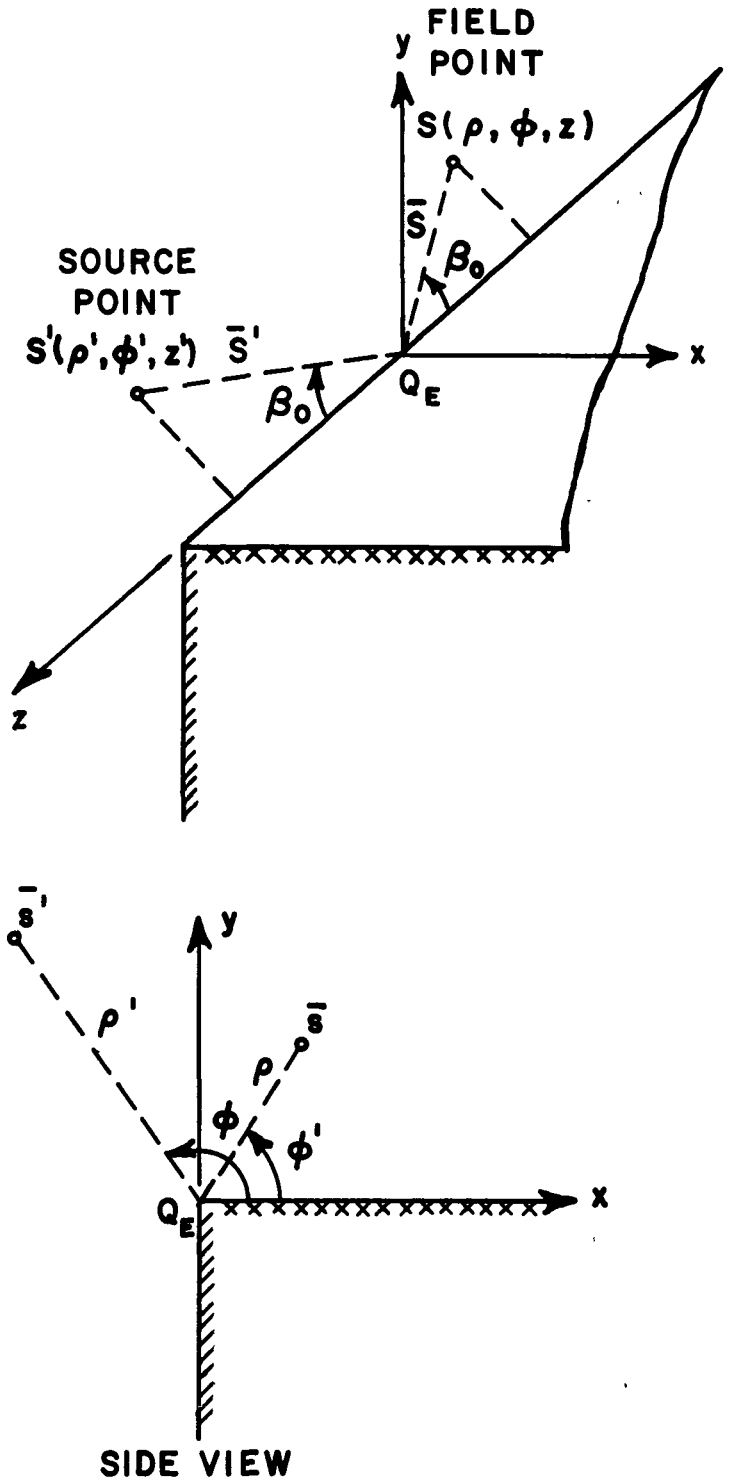

Fig. 4. Geometry for a point source illumination of a right-angled wedge.

where $k_t^2 = k^2 - h^2$.

The z-variation of the function $U_{\substack{a\\b}}$ is removed, and rewritting the above equation as

$$(49) \qquad (\nabla_t^2 + k_t^2)\, \tilde{U}_{\substack{a\\b}}(\rho,\phi,h;\bar{s}')\, e^{jhz'} = -\delta(x-x')\delta(y-y')$$

allows one to identify $\tilde{U}_{\substack{a\\b}}(\rho,\phi,h;\bar{s}')e^{jhz'}$ as $U_{\substack{a\\b}}(\bar{\rho},\bar{\rho}')$ which is a 2-dimensional scalar line source Green's function of (1), with the exception that k now is replaced by k_t in (1). Hence $\tilde{U}_{\substack{a\\b}}(\rho,\phi,h;\bar{s}')e^{jhz'}$ is replaced by $U_{\substack{a\\b}}(\bar{\rho},\bar{\rho}';k_t)$. The total field $U_{\substack{a\\b}}(\bar{s}',\bar{s}')$ is thus obtained by taking the inverse Fourier transform of $\tilde{U}_{\substack{a\\b}}(\rho,\phi,h;\bar{s}')e^{jhz'}$. It will be shown in Appendix I that

$$(50a) \qquad U^i_{\substack{a\\b}} = \frac{e^{-jk|\bar{s}-\bar{s}'|}}{4\pi|\bar{s}-\bar{s}'|} \quad ,$$

$$(50b) \qquad U^r = R\,\frac{e^{-jk|\bar{s}_i-\bar{s}'|}}{4\pi|\bar{s}_i-\bar{s}'|}$$

and

$$(50c) \qquad U^d_{\substack{a\\b}} \sim U^i\, \frac{D_{\substack{a\\b}}}{\sin\beta_o}\, \sqrt{\frac{s'}{s(s+s')}}\; e^{-jks},$$

In which

$$U^i \sim \frac{e^{-jks'}}{4\pi s'} \quad ,$$

$\bar{s}_i$ is the image point of the source $\bar{s}'$ and

$$R = \begin{cases} 1 \\ -1 \\ \dfrac{jk\sin\phi+\lambda}{jk\sin\phi-\lambda} \end{cases}$$

which depends on the boundary condition at the surface of reflection. $D_{\substack{a\\b}}$ is again given by Eq. (28) or Eq. (30) with the exception that κ is replaced by $\frac{kss'}{s+s'}\sin^2\beta_o$. The $\frac{1}{\sin\beta_o}$ factor in Eq. (50c) is to be expected because of the conical spreading of the diffracted rays due to oblique incidence from the point source. This conical spreading is a consequence of the generalized Fermat's principle.[12]

So far we have solved for the fields diffracted by a right-angled wedge due to different kinds of wave illumination, we observe that the solution of the problem of a cylindrical wave illumination is essential for the cases of plane wave and spherical wave illumination. The plane wave illumination is treated as a special case of cylindrical wave illumination when the source is removed to infinity whereas the spherical wave illumination is related to the cylindrical case by applying the Fourier transform with respect to the z-variable.

The asymptotic approximation in each case in the far zone yields a solution which can be interpreted in terms of the geometrical theory of diffraction. The pole contributions in the asymptotic approximation give the geometrical optics field which consists of the incident field and the reflected field, whereas the saddle point contribution gives the diffracted field. The geometrical optics field is discontinuous when one crosses a shadow or reflection boundary. This discontinuity in the geometrical optics field is compensated by the diffracted field. Thus the total field, which is the sum of the geometrical optics field and the diffracted field, is continuous in the whole region.

It is interesting to note that the diffraction coefficient has the same form for the different wave illuminations. The only difference for the different types of illumination is in the large parameter in the asymptotic approximation. If we let $\kappa = kL$, then

$$(51) \qquad L = \begin{cases} \rho & \text{for plane wave illumination} \\ \dfrac{\rho\rho'}{\rho+\rho'} & \text{for cylindrical wave illumination} \\ \dfrac{ss'}{s+s'}\sin^2\beta_0 & \text{for spherical wave illumination.} \end{cases}$$

In the next chapter it will be seen that the scalar diffraction coefficients D_a and D_b appear in the electromagnetic problem for plane or cylindrical waves normally incident on the edge. Furthermore it will be seen that when a ray-fixed coordinate system is introduced, the dyadic diffraction coefficient is merely the sum of two dyads or it can be expressed alternatively as a diagonalized 2x2 matrix, These properties were noted earlier in the asymptotic solution of the diffraction by a perfectly-conducting wedge[13,20].

CHAPTER III
ELECTROMAGNETIC WAVE DIFFRACTION

In Chapter II we treat the diffraction of a right-angled wedge illuminated by plane, cylindrical and spherical waves. The plane waves and the cylindrical waves associated with the uniform line source are normally incident on the edge of the wedge; the spherical wave, obliquely incident. In this chapter we show that the solutions of these scalar problems can be directly related to the corresponding electromagnetic problems provided that the electromagnetic waves are normally incident on the wedge.

First, let us introduce the ray-fixed coordinate system described in Reference [13]. As mentioned earlier, the use of this coordinate system will enable us to write the dyadic diffraction coefficients as the sum of two dyads or in the form of a 2x2 diagonal matrix.

Let us consider the field radiated from the source O and observed at P, as shown in Fig. 5. It is well known that the ray

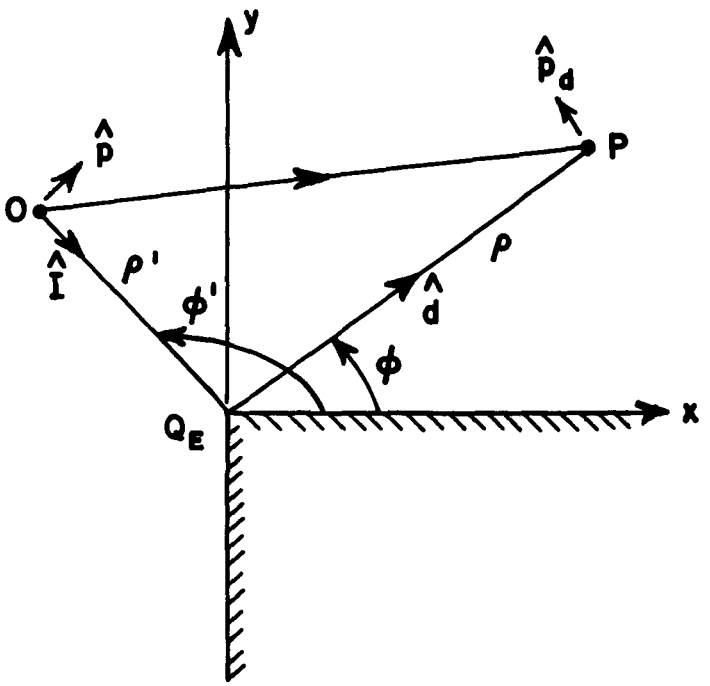

Fig. 5. Geometry for the ray coordinate system for electromagnetic wedge diffraction.

incident on the edge at Q_E in Fig. 5 gives rise to a diffracted field. To account for this Keller[12] has introduced a class of rays which includes an edge point such as Q_E on their trajectory. Applying his generalization of Fermat's principle, the distance OQ_EP along the ray path is an extremum, and the law of edge diffraction results.

Let the coordinates of the source O be (ρ',ϕ') and the observation point P be (ρ,ϕ), as shown in Fig. 5. The unit vector $\hat{d}$ is in the direction of diffraction; the unit vector $\hat{I}$ is in the direction of incidence. The unit vector $\hat{e}$ is the unit vector parallel to z-axis (the edge of the wedge). Note that $\hat{p} = \hat{e} \times \hat{I}$, $\hat{p}_d = \hat{e} \times \hat{d}$, and $\hat{e} = \hat{z}$. The orthogonal unit vectors associated with coordinates $(\rho',\phi';\rho,\phi)$ form a ray-fixed coordinate system. It will be shown later that when the incident field is decomposed into $\hat{e}$- and $\hat{p}$-directed components, and the diffracted field into $\hat{e}$- and $\hat{p}_d$-directed components, the diffraction coefficients can be expressed as a 2x2 diagonal matrix or as the sum of two dyads.

In the following sections the diffracted field components will be determined first in the edge-fixed coordinate system, $(\rho',\phi';\rho,\phi)$, which is the cylindrical coordinate system with z-axis aligned in the direction of the edge of the wedge, and then transformed to the ray-fixed coordinate system.

A. Cylindrical Wave Illumination

The diffraction of a normally incident cylindrical electromagnetic wave by a right-angled wedge is considered in this section. The direction of incidence, which is normal to the cylindrical wave fronts, is given by the unit vector $\hat{I}$. Note that $\hat{I} \cdot \hat{z} = \hat{I} \cdot \hat{e} = 0$. Cylindrical waves can be generated by a uniform electric current line source $\hat{z}I$ or uniform magnetic current line source $\hat{z}M$ located at (ρ',ϕ'), where I and M are the current amplitudes of the uniform line sources.

It can be shown that the axial incident electric field due to $\hat{z}I$ and the axial incident Magnetic field due to $\hat{z}M$ are

(52a) $$E_z^i = \frac{k^2}{j\omega\varepsilon} \; I \times \left[-\frac{j}{4} H_o^{(2)}(k\rho')\right]$$

and

(52b) $$H_z^i = \frac{k^2}{j\omega\mu} \; M \times \left[-\frac{j}{4} H_o^{(2)}(k\rho')\right],$$

respectively. The primes are used to denote the source coordinate system.

First let us consider the cylindrical wave behavior due to the uniform electric current line source. The fields due to this line source are

(53a) $$H_z^i = 0,$$

(53b) $$E_z^i = \frac{k^2}{j\omega\varepsilon} I \left[-\frac{j}{4} H_o^{(2)}(k\rho')\right].$$

(53c) $$\bar{E}_t^i = 0,$$

and

(53d) $$\bar{H}_t^i = -\hat{\phi}' \frac{j\omega\varepsilon}{k^2} \frac{\partial E_z^i}{\partial \rho'} \quad .$$

For large $k\rho'$, the Hankel function $H_o^{(2)}(k\rho')$ can be replaced by its large-argument approximation. Thus

(54a) $$\bar{E}^i \cong \hat{z} I \frac{k^2}{j\omega\varepsilon} \left[-\frac{j}{4}\sqrt{\frac{2}{\pi k\rho'}} e^{-j(k\rho' - \frac{\pi}{4})}\right] \quad ,$$

and

(54b) $$\bar{H}^i \cong \hat{\phi}' jIk \left[-\frac{j}{4}\sqrt{\frac{2}{\pi k\rho'}} e^{-j(k\rho' - \frac{\pi}{4})}\right] .$$

The equation $k\rho' = \text{constant}$, describes a cylindrical surface. The direction of incidence

$$\hat{I} = -\hat{\rho}'. \tag{55}$$

and

$$\hat{I} \cdot \bar{E}^i = 0, \tag{56a}$$

$$\hat{I} \cdot \bar{H}^i = 0; \tag{56b}$$

hence in the far zone, the EM field is a cylindrical wave with its field vectors tangent to the wavefront, and perpendicular to its associated rays. The EM field of a uniform magnetic current line source can be shown to have the same properties.

The total axial fields (E_z and H_z) excited by uniform electric and uniform magnetic current line sources can be shown to be

$$E_z = \frac{k^2}{j\omega\varepsilon} I\, U_a(\bar{\rho},\bar{\rho}') \tag{57a}$$

and

$$H_z = \frac{k^2}{j\omega\mu} M\, U_b(\bar{\rho},\bar{\rho}'), \tag{57b}$$

respectively. The special function $U_{\substack{a\\b}}(\bar{\rho},\bar{\rho}')$ is the same as that of Eq. (1). The solution of Eq. (1) is given in Eq. (23). By substituting the integral representations of Green's function G and W, shown in Appendix I, into Eq. (23), it becomes

$$U_{\substack{a\\b}}(\bar{\rho},\bar{\rho}') \simeq e^{-jk(\rho+\rho')} \int_{L-L'} F_{\substack{a\\b}}(\xi,\phi,\phi') \sqrt{\frac{2}{j\pi k(\rho^2+\rho'^2-2\rho\rho'\cos\xi)^{1/2}}}\ x \tag{58}$$

$$x\ e^{\kappa f(\xi)}\, d\xi\ ,$$

where

$$(59a)\qquad F_a(\xi,\phi,\phi') = \frac{1}{6\pi j(\lambda - jk\sin\phi)}\left\{\lambda\left[\cot\left(\frac{\xi+\beta^-}{3}\right) - \cot\left(\frac{\xi+\beta^+}{3}\right) - jk\sin\phi\left[\sin\left(\frac{\xi+\beta^-}{3}\right) + \sin\left(\frac{\xi+\beta^+}{3}\right)\right] + \frac{\cos^2\left(\frac{\xi+\beta^-}{3}\right)}{\sin\left(\frac{\xi+\beta^-}{3}\right)} + \frac{\cos^2\left(\frac{\xi+\beta^+}{3}\right)}{\sin\left(\frac{\xi+\beta^+}{3}\right)}\right]\right\}$$

and

$$(59b)\qquad F_b(\xi,\phi,\phi') = \frac{1}{6\pi j(\lambda - jk\sin\phi)}\left\{\lambda\left[\sin\left(\frac{\xi+\beta^-}{3}\right) - \sin\left(\frac{\xi+\beta^+}{3}\right) + \frac{\cos^2\left(\frac{\xi+\beta^-}{3}\right)}{\sin\left(\frac{\xi+\beta^-}{3}\right)} - \frac{\cos^2\left(\frac{\xi+\beta^+}{3}\right)}{\sin\left(\frac{\xi+\beta^+}{3}\right)}\right] - jk\sin\phi\ x\ x\left[\cot\left(\frac{\xi+\beta^-}{3}\right) + \cot\left(\frac{\xi+\beta^+}{3}\right)\right]\right\} .$$

Note that $\beta^{\pm} = \phi \pm \phi'$, $f(\xi) = j(1+\cos\xi)$ and $\kappa = \frac{k\rho\rho'}{\rho+\rho'}$.

The diffracted ray contribution to Eq. (58) is known from the result of Eq. (A-36) in Appendix I. Thus the axial diffracted fields can be written as

$$(60a)\qquad E_z^d \sim E_z^i\, D_a \frac{e^{-jk\rho}}{\sqrt{\rho}} \quad ,$$

and

$$(60b)\qquad H_z^d \sim H_z^i\, D_b \frac{e^{-jk\rho}}{\sqrt{\rho}} \quad ,$$

where E_z^i and H_z^i are given by Eqs. (52a) and (52b) with the Hankel function replaced by its large argument approximation, and D_a and D_b are given by Eqs. (28) and (30), respectively.

For a problem which possesses cylindrical uniformity in structure and fields, the transverse fields $\bar{E}_t$ and $\bar{H}_t$ can be determined from the longitudinal fields E_z and H_z using the following relations

$$\text{(61a)} \qquad \bar{E}_t = - jk_z \frac{\nabla_t E_z}{k^2-k_z^2} + j\omega\mu \frac{\hat{z} \times \nabla_t H_z}{k^2-k_z^2}$$

and

$$\text{(61b)} \qquad \bar{H}_t = - jk_z \frac{\nabla_t H_z}{k^2-k_z^2} - j\omega\varepsilon \frac{\hat{z} \times \nabla_t E_z}{k^2-k_z^2} \quad ,$$

where $k^2 = k_t^2 + k_z^2$. In the case of a normally incident EM wave, $k_t = k$ and $k_z = 0$.

To evaluate $\bar{E}_t$ and $\bar{H}_t$, it is first assumed that we can interchange the order of integration and differentiation when $\hat{z} \times \nabla_t$ operates on the integral, Eq. (58). Since only those terms of $O(\frac{1}{\sqrt{\rho}})$ are retained in the asymptotic evaluation of the integral, the approximation $\nabla_t \simeq \frac{\partial}{\partial \rho} \hat{\rho}$ is made. Thus

$$\text{(62a)} \qquad \nabla_t E_z \sim \hat{\rho}\, E_z^i\, e^{-jk(\rho+\rho')} \int_{L-L'} -jk\, F_a(\xi,\phi,\phi') \times \sqrt{\frac{2}{j\pi k(\rho^2+\rho'^2-2\rho\rho'\cos\xi)^{1/2}}}\, e^{\kappa f(\xi)}\, d\xi$$

and

$$(62b)\qquad \nabla_t H_z \sim \hat{\rho}\, H_z^i\, e^{-jk(\rho+\rho')} \int_{L-L'} -jk\, F_b(\xi,\phi,\phi') \times$$

$$\times \sqrt{\frac{2}{j\pi k(\rho^2+\rho'^2-2\rho\rho'\cos\xi)^{1/2}}}\; e^{\kappa f(\xi)}\, d\xi\ .$$

The diffracted field contribution to $\nabla_t E_z$ and $\nabla_t H_z$ is then obtained from the asymptotic approximation of the above integrals via the modified method of steepest descent with the result that

$$(63)\qquad \begin{bmatrix} \nabla_t E_z^d \\ \nabla_t H_z^d \end{bmatrix} \sim \hat{\rho}\,(-jk)\, \begin{matrix} D_a \\ b \end{matrix} \frac{e^{-jk\rho}}{\sqrt{\rho}} \begin{bmatrix} E_z^i \\ H_z^i \end{bmatrix}$$

where D_a in the above equation are identical to D_a in Eqs. (60a) and (60b). Substituting Eq. (63) into Eqs. (61a) and (61b), we obtain the transverse fields

$$(64a)\qquad \bar{E}_t = (\bar{E}^i \cdot \hat{p})\, \hat{p}_d\, D_b \frac{e^{-jk\rho}}{\sqrt{\rho}}$$

and

$$(64b)\qquad \bar{H}_t = (\bar{H}^i \cdot \hat{p})\, \hat{p}_d\, D_a \frac{e^{-jk\rho}}{\sqrt{\rho}}\ .$$

In deriving the above equations, we have used $\bar{H}^i \cdot \hat{p} = -y_o\, \hat{z}\, E_z^i$ for a uniform electric current line source and $\bar{E}^i \cdot \hat{p} = z_o\, \hat{z}\, H_z^i$ for a uniform magnetic current line source.

Thus the diffracted field for a uniform cylindrical electromagnetic wave normally incident on the wedge is

$$(65a)\qquad \bar{E}^d = (\bar{E}^i \cdot \hat{z})\, \hat{z}\, D_a \frac{e^{-jk\rho}}{\sqrt{\rho}}$$

and

$$\text{(65b)} \qquad \bar{H}^d = (\bar{H}^i \cdot \hat{p})\, \hat{p}_d\, D_a\, \frac{e^{-jk\rho}}{\sqrt{\rho}} \quad ,$$

whereas the diffracted field for a uniform cylindrical electromagnetic wave normally incident on the wedge is

$$\text{(66a)} \qquad \bar{E}^d = (\bar{E}^i \cdot \hat{p})\, \hat{p}_d\, D_b\, \frac{e^{-jk\rho}}{\sqrt{\rho}}$$

and

$$\text{(66b)} \qquad \bar{H}^d = (\bar{H}^i \cdot \hat{z})\, \hat{z}\, D_b\, \frac{e^{-jk\rho}}{\sqrt{\rho}} \quad .$$

Let us define two dyads $\bar{\bar{D}}_E$ and $\bar{\bar{D}}_H$ such that

$$\text{(67a)} \qquad \bar{\bar{D}}_E = \hat{e}\,\hat{e}\, D_a + \hat{p}\,\hat{p}_d\, D_b$$

and

$$\text{(67b)} \qquad \bar{\bar{D}}_H = \hat{e}\,\hat{e}\, D_b + \hat{p}\,\hat{p}_d\, D_a,$$

We can rewrite Eqs. (65) and (66) in the form of the geometrical theory of diffraction:

$$\text{(68a)} \qquad \bar{E}^d \sim \bar{E}^i(Q_E) \cdot \bar{\bar{D}}_E\, \frac{e^{-jk\rho}}{\sqrt{\rho}}$$

and

$$\text{(68b)} \qquad \bar{H}^d \sim \bar{H}^i(Q_E) \cdot \bar{\bar{D}}_H\, \frac{e^{-jk\rho}}{\sqrt{\rho}} \quad .$$

Alternatively, expressing the diffraction coefficients in matrix notation, we can write:

$$(69a)\qquad \begin{bmatrix} E_{\parallel}^{d} \\ E_{\perp}^{d} \end{bmatrix} \sim \begin{bmatrix} D_a & 0 \\ 0 & D_b \end{bmatrix} \begin{bmatrix} E_{\parallel}^{i}(Q_E) \\ E_{\perp}^{i}(Q_E) \end{bmatrix} \frac{e^{-jk\rho}}{\sqrt{\rho}}$$

and

$$(69b)\qquad \begin{bmatrix} H_{\perp}^{d} \\ H_{\parallel}^{d} \end{bmatrix} \sim \begin{bmatrix} D_b & 0 \\ 0 & D_a \end{bmatrix} \begin{bmatrix} H_{\perp}^{i}(Q_E) \\ H_{\parallel}^{i}(Q_E) \end{bmatrix} \frac{e^{-jk\rho}}{\sqrt{\rho}} \quad ,$$

where $E_{\parallel}^{d} = \bar{E}^{d} \cdot \hat{e}$, $E_{\perp}^{d} = \bar{E}^{d} \cdot \hat{p}_d$, $E_{\parallel}^{i}(Q_E) = \bar{E}^{i}(Q_E) \cdot \hat{e}$, and $E_{\perp}^{i}(Q_E) = \bar{E}^{i}(Q_E) \cdot \hat{p}$; $H_{\perp}^{d} = \bar{H}^{d} \cdot \hat{e}$, $H_{\parallel}^{d} = \bar{H}^{d} \cdot \hat{p}_d$, $H_{\perp}^{i}(Q_E) = \bar{H}^{i}(Q_E) \cdot \hat{e}$, and $H_{\parallel}^{i}(Q_E) = \bar{H}^{i}(Q_E) \cdot \hat{p}$. Thus the matrix in the above equations is diagonal because the components of the field components are expressed in the proper coordinate system for the problem and only the terms of $O(\frac{1}{\sqrt{\rho}})$ are retained.

B. Plane Wave Illumination

For an electromagnetic plane wave normally incident on the edge of the wedge, the total electric field is given by

$$(70a)\qquad \bar{E} = \hat{z}\, E^{i}\, U_a^p$$

for an incident electric plane wave field $\hat{z}\, E^{i}$, whereas the total magnetic field is given by

$$(70b)\qquad \bar{H} = \hat{z}\, H^{i}\, U_b^p$$

for an incident magnetic plane wave field $\hat{z}\, H^{i}$, where $U_{\substack{a \\ b}}^{p}$ is the solution of Eq. (43) and is given as

$$(71) \qquad U_{a\,b}^{p} = \int_{L-L'} F_{a\,b}\,(\xi,\phi,\phi')\, e^{jk\rho\cos\xi}\, d\xi$$

with $F_{a\,b}\,(\xi,\phi,\phi')$ given by Eqs. (59a) and (59b).

The diffracted ray contribution can then be obtained by asymptotically evaluating the integrals, Eq. (71), via the modified method of steepest descent. Thus,

$$(72a) \qquad E_z^d \sim E_z^i\, D_a\, \frac{e^{-jk\rho}}{\sqrt{\rho}}$$

and

$$(72b) \qquad H_z^d \sim H_z^i\, D_b\, \frac{e^{-jk\rho}}{\sqrt{\rho}} \quad ,$$

where E_z^i and H_z^i are evaluated at Q_E, the point of incidence on the edge, and $D_{a\,b}$ are given in Eq. (28) and Eq. (30) with the exception that $\kappa = k\rho$ in the large argument parameter.

The transverse components of the diffracted fields can be computed in the manner similar to that of the cylindrical wave case treated in the last section. Following the same procedure, we obtain

$$(73a) \qquad \bar{E}^d \sim \bar{E}^i(Q_E) \cdot \bar{\bar{D}}_E\, \frac{e^{-jk\rho}}{\sqrt{\rho}}$$

and

$$(73b) \qquad \bar{H}^d \sim \bar{H}^i(Q_E) \cdot \bar{\bar{D}}_H\, \frac{e^{-jk\rho}}{\sqrt{\rho}}$$

where $\bar{\bar{D}}_E$ and $\bar{\bar{D}}_H$ are exactly the same as those given in Eqs. (68a) and (68b), except that κ is equal to $k\rho$ in this case.

Summarizing the results obtained thus far, the diffracted electric field can be written as

$$\bar{E}^d(s) \approx \bar{E}^i(Q_E) \cdot \bar{\bar{D}}_E(\hat{s},\hat{I})\, A(s)\, e^{-jks}, \tag{74}$$

where $\bar{E}^i(Q_E)$ is the incident electric field at the point of diffraction, $A(s)$ is the spatial attenuation which describes how the field intensity varies along the diffracted ray,

$$A(s) = \frac{1}{\sqrt{s}} \qquad \text{for plane and cylindrical wave incidence.} \tag{75}$$

$\bar{\bar{D}}_E(\hat{s},\hat{I})$ is the dyadic diffraction coefficient,

$$\bar{\bar{D}}_E = \hat{z}\hat{z}\, D_a + \hat{p}\hat{p}_d\, D_b, \tag{76}$$

where

$$D_a = \frac{\lambda_a D_s - jk\sin\phi\, D_{g1}}{\lambda_a - jk\sin\phi} \tag{77a}$$

and

$$D_b = \frac{\lambda_b D_{g2} - jk\sin\phi\, D_h}{\lambda_b - jk\sin\phi} \tag{77b}$$

where

$$D_{\substack{s\\h}} = \left[\left\{d^+(\beta^-)F[ka^+(\beta^-)] + d^-(\beta^-)F[ka^-(\beta^-)]\right\} \mp \mp \left\{d^+(\beta^+)F[ka^+(\beta^+)] + d^-(\beta^+)F[ka^-(\beta^+)]\right\}\right], \tag{78}$$

and

$$D_{\substack{g1\\g2}} = -\frac{e^{-j\frac{\pi}{4}}}{3\sqrt{2\pi k}}\left[2\sin\frac{\pi}{3}\left(\cos\frac{\beta^-}{3} \pm \cos\frac{\beta^+}{3}\right) + \left\{d_g^+(\beta^-)F[ka^+(\beta^-)] + d_g^-(\beta^-)F[ka^-(\beta^-)]\right\} \pm \pm \left\{d_g^+(\beta^+)F[ka^+(\beta^+)] + d_g^-(\beta^+)F[ka^-(\beta^+)]\right\}\right], \tag{79}$$

$$(80) \qquad d^{\pm}(\beta) = -\frac{e^{-j\frac{\pi}{4}}}{3\sqrt{2\pi k}} \cot\left(\frac{\pi \pm \beta}{3}\right) ,$$

$$(81) \qquad d_g^{\pm}(\beta) = \frac{\cos^2\left(\frac{\pi \pm \beta}{3}\right)}{\sin\left(\frac{\pi \pm \beta}{3}\right)} ,$$

in which $\beta = \beta^{\pm} = \phi \pm \phi'$ and

$$(82) \qquad F[\kappa a^{\pm}(\beta)] = 2j\left|\sqrt{\kappa a^{\pm}(\beta)}\right| e^{j\kappa a^{\pm}(\beta)} \int_{\left|\sqrt{\kappa a^{\pm}(\beta)}\right|}^{\infty} e^{-jt^2}\, dt.$$

The parameters which appear in $F(\kappa a^{\pm}(\beta))$ are

$$(83) \qquad a^{\pm}(\beta) = 1 + \cos(-\beta + 3N^{\pm}\pi)$$

in which $N^{\pm}$ is the positive or negative integer whih most closely satisfies the equations:

$$(84) \qquad \begin{cases} 3\pi N^{+} - \beta = \pi \\ 3\pi N^{-} - \beta = -\pi . \end{cases}$$

The quantity $\kappa = kL$ is the large parameter in the asymptotic evaluation of the pertinent intergrals involved in the formulation of the dyadic diffraction coefficient. The quantity L is given by

$$(85) \qquad L = \begin{cases} \rho & \text{for plane wave illumination} \\ \frac{\rho\rho'}{\rho+\rho'} & \text{for cylindrical wave illumination.} \end{cases}$$

When the ray-fixed coordinate system is employed, the dyadic diffraction coefficient can be expressed as the sum of two dyads. One of the dyads involves D_a, the scalar diffraction coefficient for

TE (to $\hat{z}$) case; and the other, D_b, for TM (to $\hat{z}$) case. In turn, D_a and D_b are composed of trigonometric functions which are given by $d(\beta)$ and $d_g(\beta)$ and $F(\kappa a^{\pm}(\beta))$ which involves the Fresnel integral. The latter can be regarded as a transition function which plays the most important role in the transition region of the reflection and shadow boundaries. The geometrical optics field is discontinuous across the reflection and shadow boundaries. It is this transition function which compensates for the discontinuity of the geometrical optics field and makes the total field continuous. Outside the transition region, $\kappa a^{\pm}(\beta) > 10$, F is approximately equal to 1. Curves of the magnitude and phase of F as a function of kLa are shown in Fig. 6. The scalar diffraction coefficients in the dyadic diffraction coefficient are independent of the wavefront of the incident field outside the transition region, as they are in the case of the perfectly-conducting wedge.

CHAPTER IV
APPLICATIONS AND NUMERICAL RESULTS

The purpose of this chapter is to show that the diffraction coefficients and the analysis described in the preceding chapters are consistent with results obtained elsewhere for some special cases of our problem. The radiation from a magnetic line source located close to the reactive surface of a right-angled wedge and the radiation from slots in truncated, dielectric-covered surfaces are considered. In both cases, the calculated and measured patterns are in good agreement. Also some calculated patterns are presented to show the effect of surface impedance on wedge diffraction. We begin with the diffraction of an electromagnetic wave by a perfectly-conducting wedge.

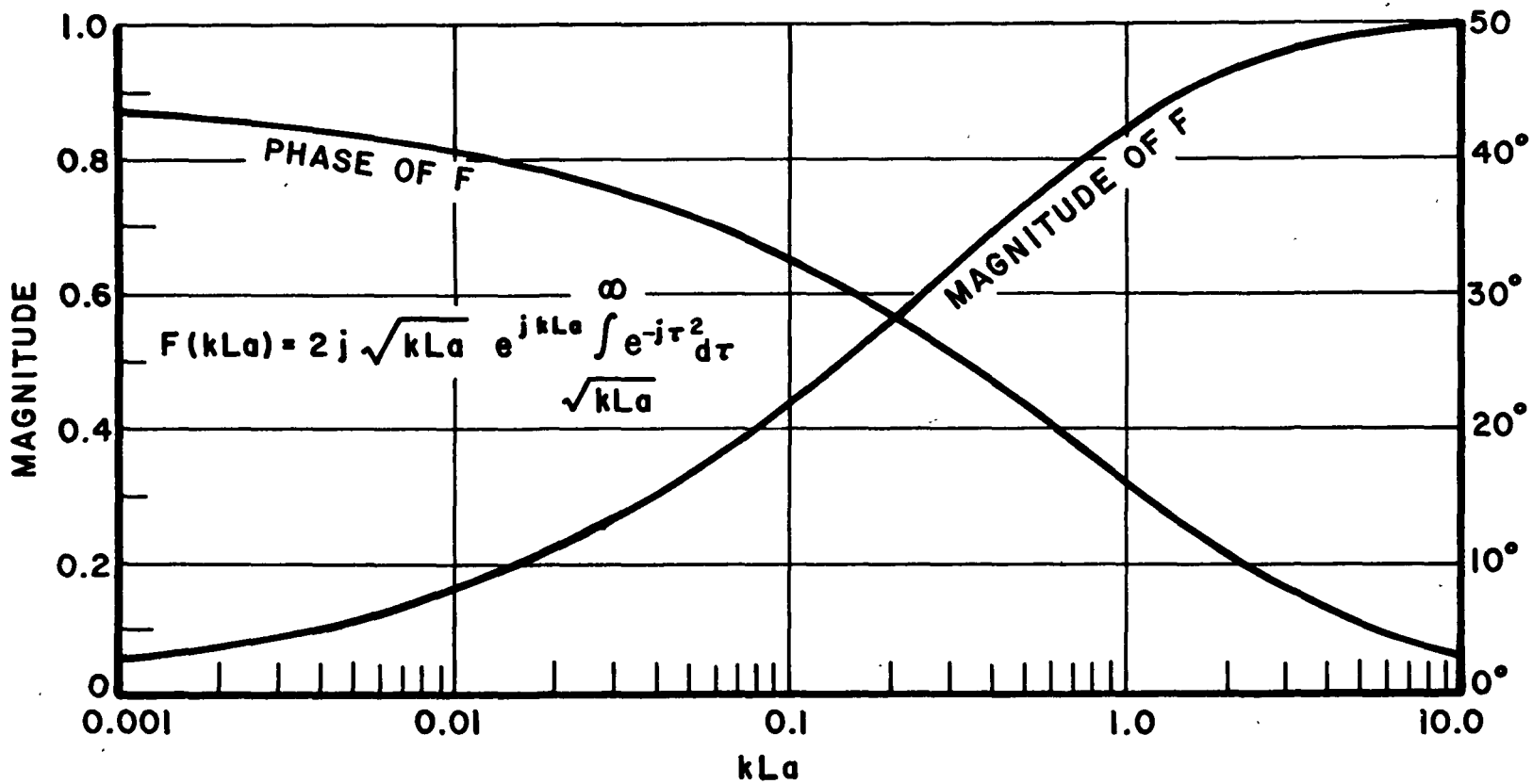

Fig. 6. Transition function F(kLa).

1. The Perfectly-conducting Wedge

A dyadic diffraction coefficient for the perfectly-conducting wedge has been derived by Pathak and Kouyoumjian[20]. Our impedance surface reduces to a perfectly-conducting surface when $\lambda_a \to -\infty$ and $\lambda_b = 0$. In Eq. (28), it is quite obvious that when $\lambda_a \to -\infty$, $D_a \to D_s$, which is their soft wedge diffraction coefficient for the right-angled wedge, and in Eq. (30), when $\lambda_b = 0$, $D_b = D_h$, which is their diffraction coefficient for a hard right-angled wedge. Thus the form of the dyadic diffraction coefficient, see Eq. (76), is the same for the impedance loaded wedge and the perfectly-conducting wedge, and so it follows that our solution reduces to that of the perfectly-conducting wedge[20].

2. Vertex-excited Surface Waves on one Face of a Right-angled Wedge

When one wedge surface supports surface waves, Re $\lambda > 0$. For the line source placed precisely at the edge of the wedge, $x'=y'=0$. The first term in the series $\frac{\partial}{\partial y'} G_b$ becomes singular. Thus the factor C-1, which is zero, multiplied by a singular term becomes an undetermined constant. Let the constant be C_1 and Eq. (16) becomes

$$V = j \frac{k}{3} H_{\frac{1}{3}}^{(2)}(kr)\cos\theta + C_1 H_{\frac{1}{3}}^{(2)}(kr)\cos\frac{\theta}{3}, \tag{86}$$

where $$\theta = \frac{3\pi}{2} - \phi.$$

The above equation was also derived in a different way by Karp and Karal[9] with a different constant coefficient in the first term; their coefficient was given as jk/4. It can be shown that when $\lambda \to 0$, $C_1 \to 0$. Thus V should reduce to the Green's function for a magnetic line source located at the tip of a perfectly-conducting right angle wedge, which is $j\frac{k}{3} H_{\frac{1}{3}}^{(2)}(kr) \cos\theta$. For this reason we believe that our coefficient for the first term is the correct one.

3. A Magnetic Current Line Source Exciting a Right-angled Wedge

In this section the radiation from a magnetic current line source located close to the reactive surface and far from the edge of the wedge is considered. The geometry is depicted in Fig. 7. The

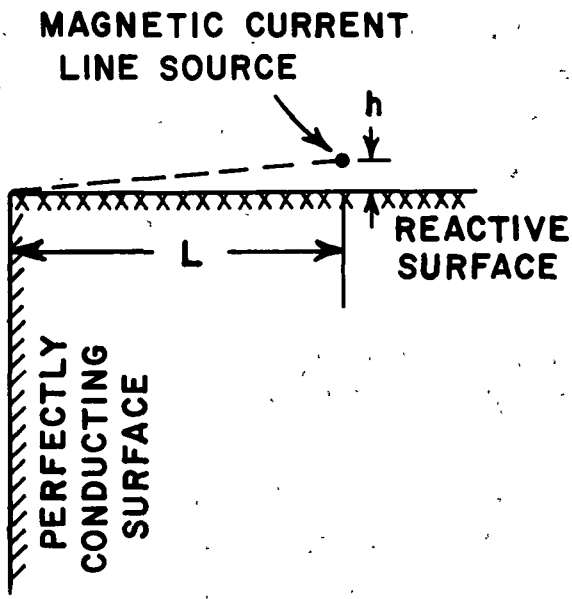

Fig. 7. Geometry of a line source radiating in the presence of a right-angled wedge.

reactive surface is such that it supports a surface wave. Since it is assumed that the magnetic current line source is quite a few wavelengths from the edge, i.e., the exciting source is located in the far zone of the scattering from the edge, as noted in Section A of Chapter II, the total radiation field is the superposition of the geometrical optics fields and the diffracted field due to the rays incident on the edge and that due to the excited surface wave. Thus Eq. (42) is used to compute the radiation pattern.

Chu[1] has considered this problem by using reciprocity in conjunction with an exact solution and the approximations involved in

the superposition. It is interesting to note that the expressions of the total radiation field are exactly the same except that the diffracted field, U^d, due to the rays incident on the edge was not yet determined and neglected in his study. Figure 8 and Fig. 9 show

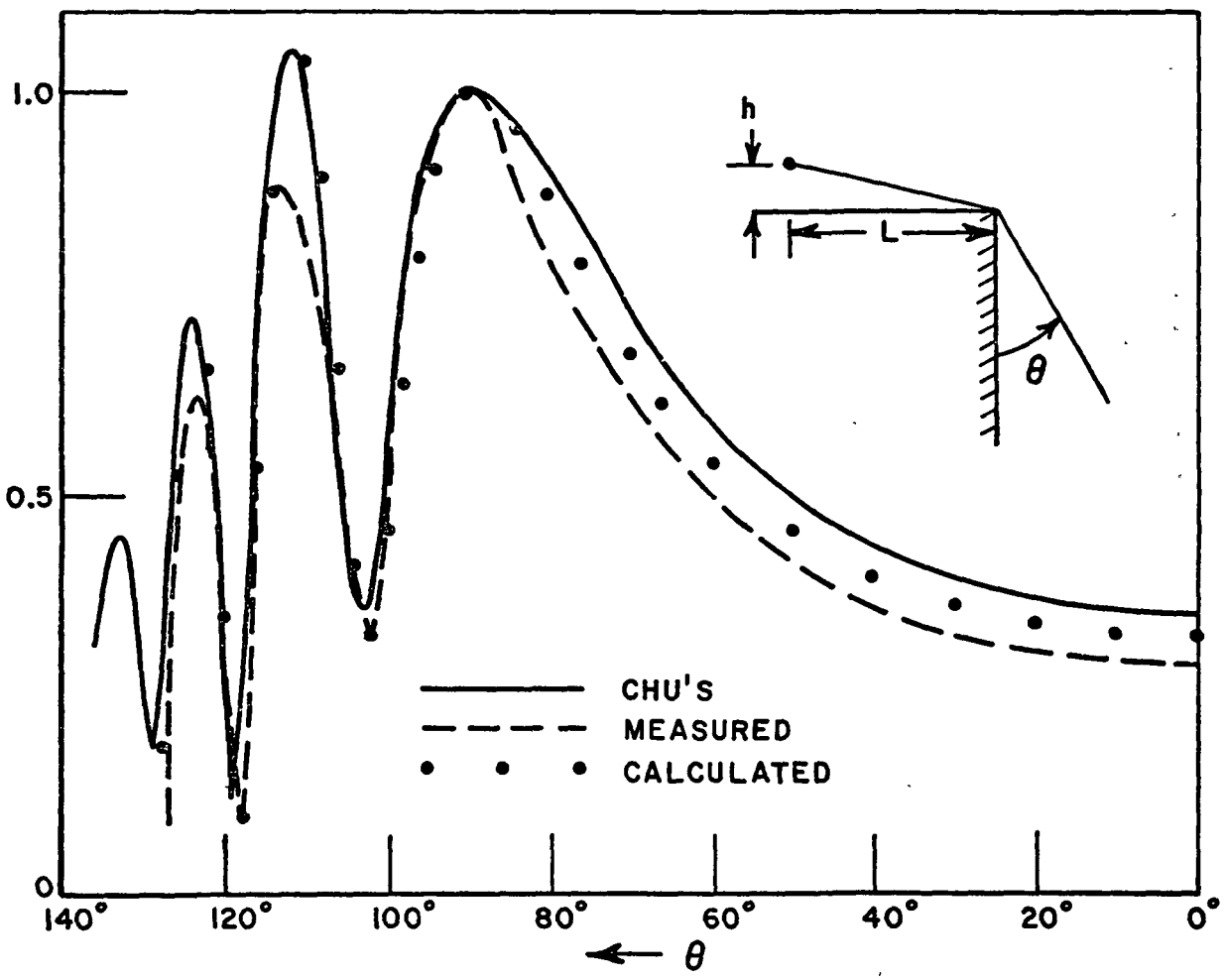

Fig. 8. The amplitude pattern of a magnetic current line source exciting a right-angled wedge. ($\beta/k=1.05$, $L=10\lambda$, $kh=1.5625$)

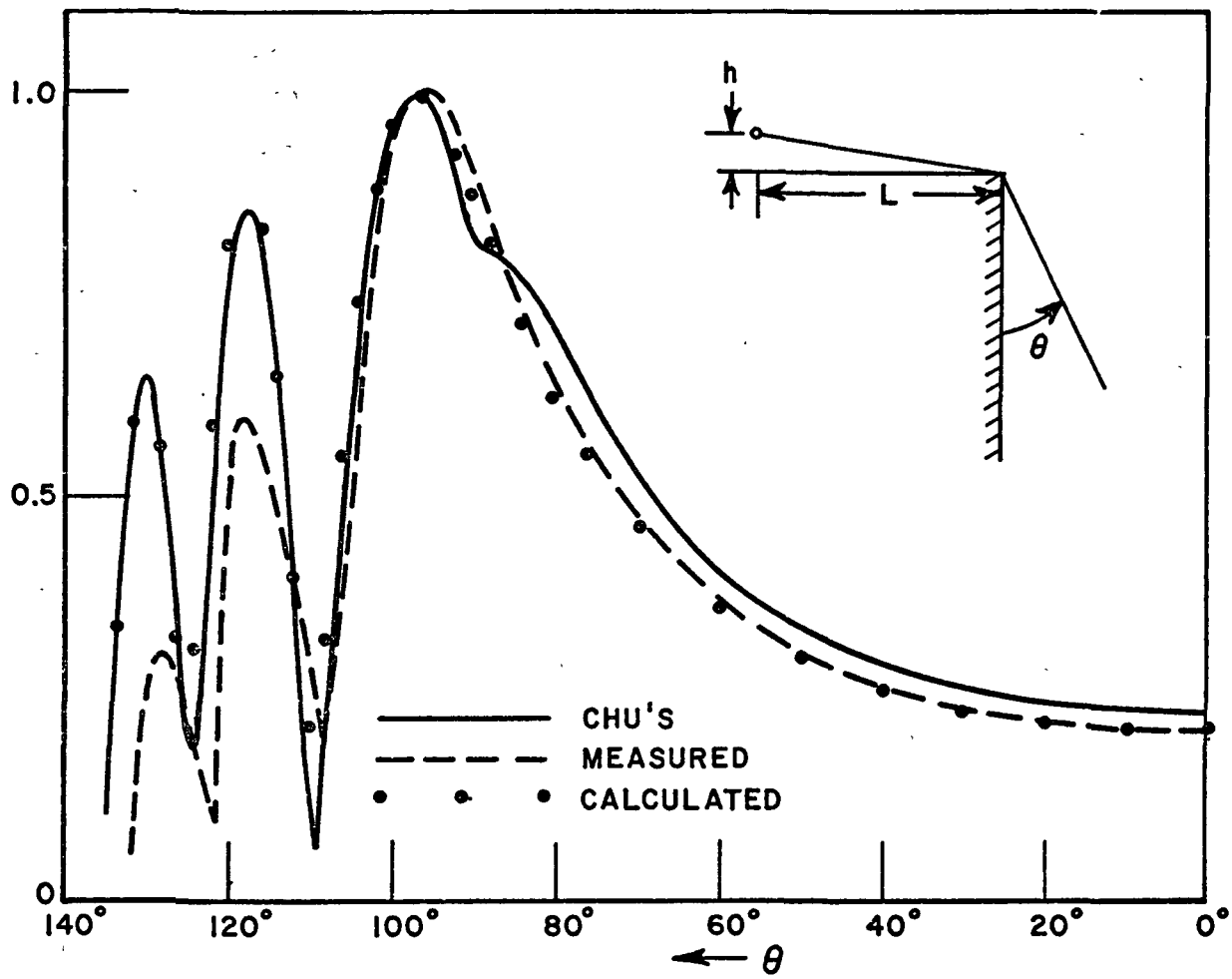

Fig. 9. The amplitude pattern of a magnetic current line source exciting a right-angled wedge. ($\beta/k=1.033$, $L=8.34\lambda$, $kh=1.309$)

the calculated patterns by Eq. (42) and those calculated and measured by Chu[1]. The improvement by including the contribution of U^d is evident in both cases. The ripple shown by Chu's computation in Fig. 9 disappears because the contribution of U^d becomes more important when the magnetic current line source is closer to the edge. The radiation field pattern of a right-angled wedge with a reactive surface ($\beta(k = 1.05)$) and that of a perfectly-conducting wedge are shown in Fig. 10. The wedge is illuminated by a magnetic current line source

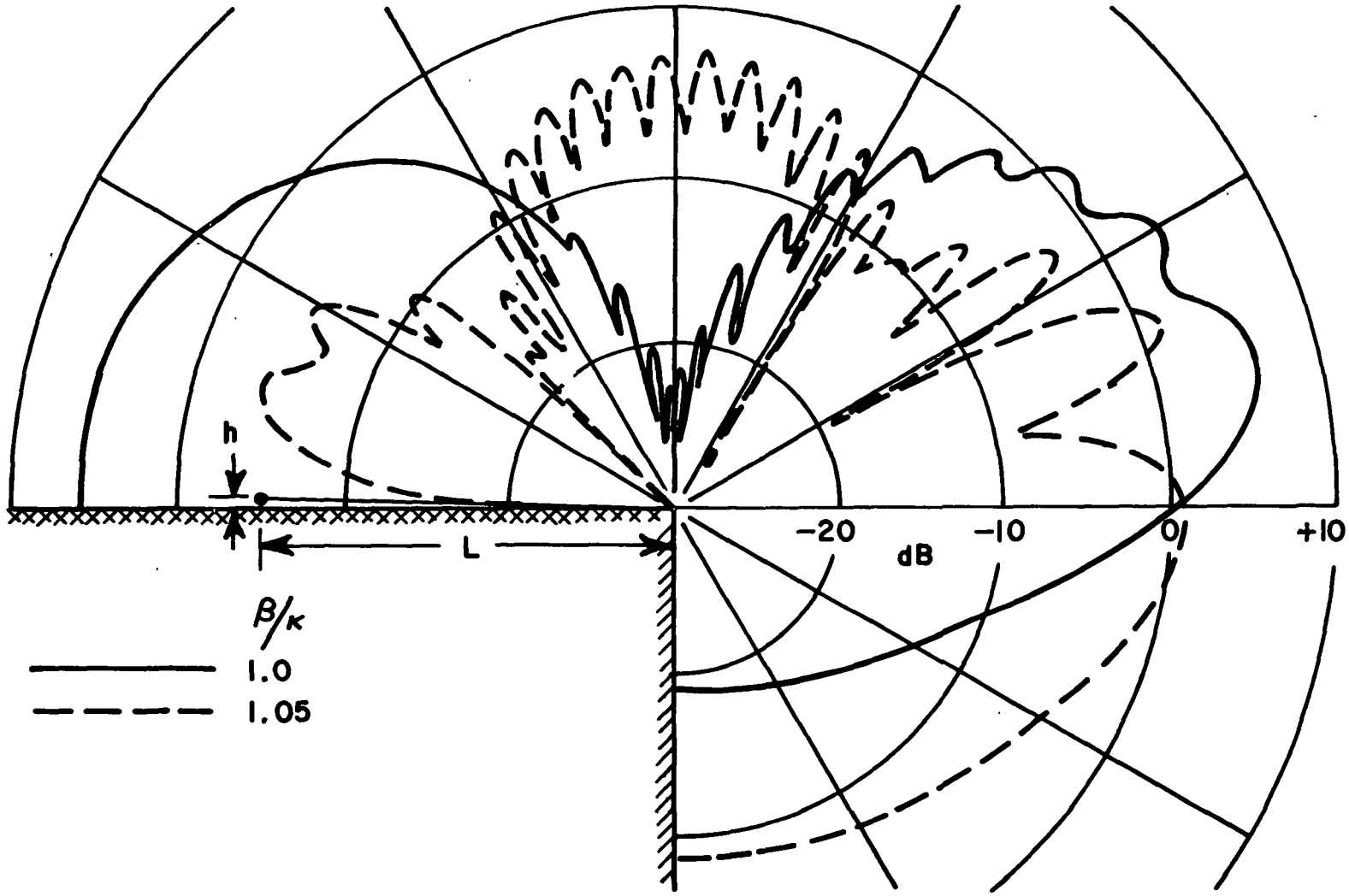

Fig. 10. The radiation pattern of a magnetic current line source. (L=10λ, kh=1.5625)

located at L = 10λ and kh = 1.5625. The increase of the radiation field in the shadow region of the wedge with a uniform impedance surface is due to the fact that the energy stored in the trapped surface wave is radiated by the termination of the edge of the wedge.

4. The Radiation from Slots in Truncated Dielectric-covered Surface

Recently, Hwang et al studied the radiation from slots in a truncated, dielectric-covered surface[6]; in particular they considered a narrow slot in the configuration depicted in Fig. 11.

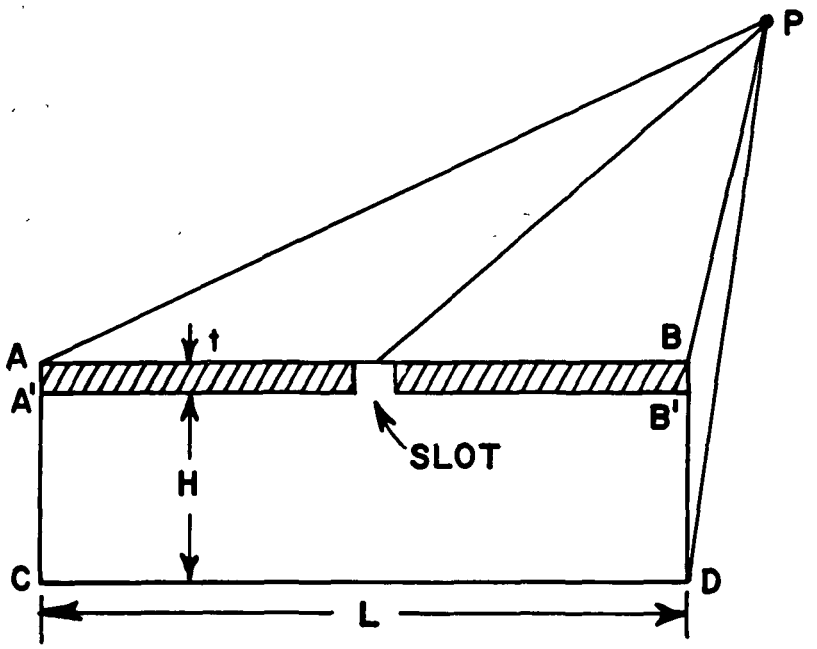

Fig. 11. The rays emanating from a slot in a dielectric-covered ground plane.

Employing the geometrical theory of diffraction, the far-zone field is the sum of a geometrical optics field and a diffracted field. The geometrical optics field is the direct radiation from the slot to the field point P; it vanishes in the shadow region below the plane containing the surface AB. The slot also excites surface waves which are

incident at the termination of the dielectric cover at A and B. For simplicity the thickness t of the dielectric cover is restricted so that only the dominant TM_0 surface mode is incident. The surface waves produce rays singly-diffracted from A and B to the field point P and to the lower edges C and D. They also produce reflected surface waves at these terminations. The contributions from the singly-diffracted rays and all significant multiply-diffracted rays are summed to give the field at P.

The canonical problem for diffraction from edges A and B is the surface wave diffraction from a right-angle wedge, one of whose faces is perfectly-conducting, while the other is an impedance surface. The canonical problem of the diffraction of a surface wave on this right-angle wedge[2] is used to find the diffraction and reflection coefficients, which are adequate for sufficiently thin dielectric covers. However, the radiation from the vertical end faces AA' (or BB') of the dielectric cover cannot be neglected in treating the thicker dielectric covers, i.e., the radiation from the field inside the slab can no longer be neglected at its termination. The effect can be taken into account by a Kirchhoff approximation using the surface wave field along the vertical end faces of the slab. The problem is then treated as the radiation from a magnetic line current distribution on the perfectly-conducting surface of a right-angle wedge whose other surface is an impedance boundary. This contributes a second term to the diffraction coefficient previously obtained. In Fig. 11, the ground plane length L is 12.12 inches, the height H is 1.71 inches, and the width is 22 inches. A 0.5 inch by 0.062 inch slot is positioned 0.1 inch to the right of the center of the ground plane, introducing a slight asymmetry in the pattern. The calculated and measured patterns are shown in Fig. 12; the two patterns are seen to be in good agreement.

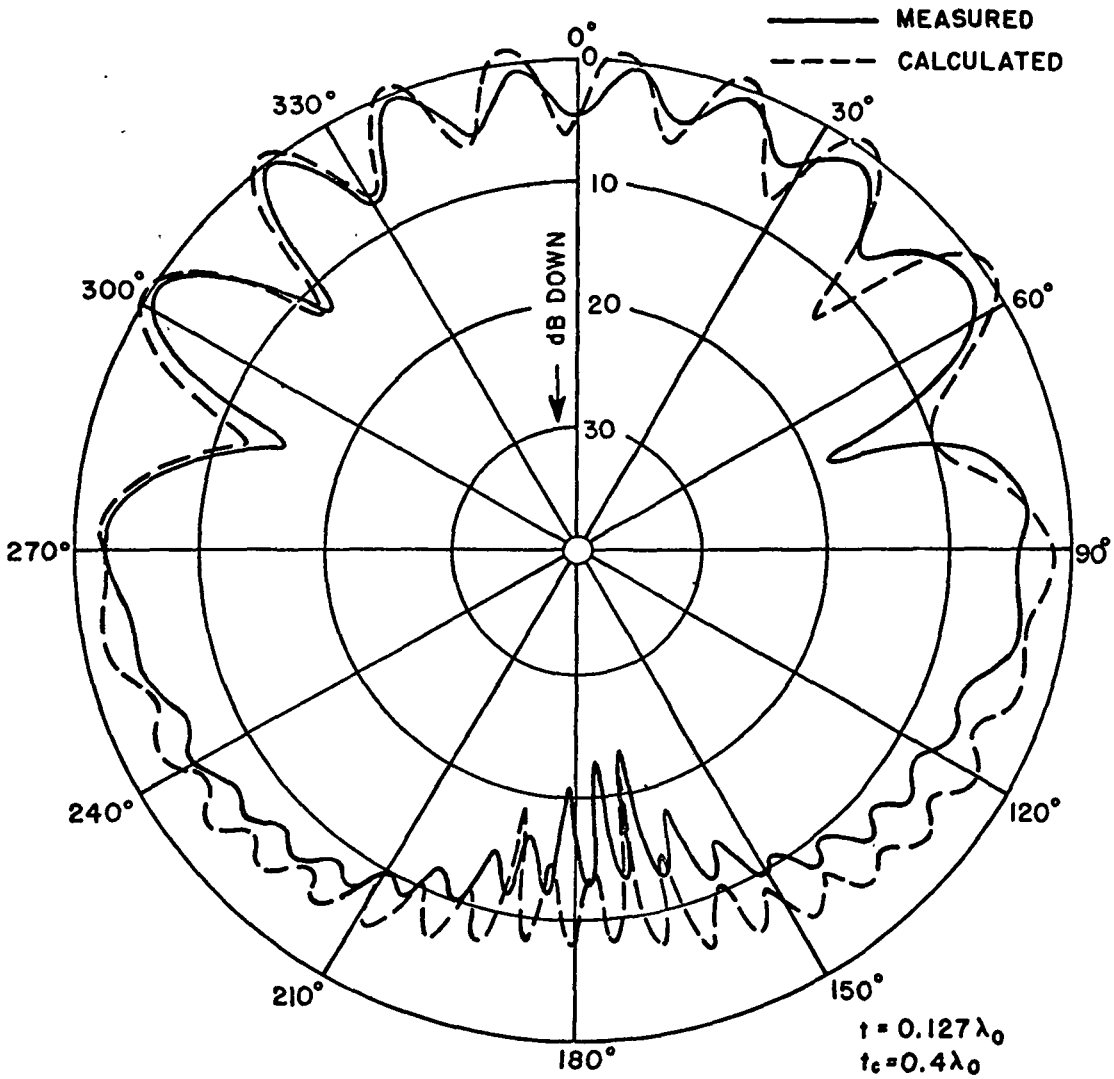

Fig. 12. Pattern of a slot in a dielectric-covered ground plane. Frequency = 8 GHz. t = 0.1875 inch, ε_r = 2.56.

5. Calculated Patterns of Impedance Loaded Wedges

We conclude this chapter by presenting some numerical results which show the effect of the diffracted field and surface impedance on edge diffraction.

It is shown in Fig. 13 that the diffracted field properly compensates for the discontinuity in the geometrical optics fields, the incident field and the reflected field, across the transition boundaries, thereby yielding a total field which is continuous everywhere.

Figures 14 through 16 show the radiation patterns of a magnetic current line source illuminating a right-angled wedge. In each case, a magnetic line source illuminates the wedge from a distance $\rho' = 1\lambda$ (wavelength) and at different ϕ' locations. The normalized surface impedance, λ_b/k, is chosen to be 0, 0.1 and 0.5. The case $\lambda_b/k = 0$ corresponds to that of a perfectly-conducting wedge. It can be seen from these patterns that when the reactance surface is in the illuminated region, the side lobe in the vicinity of the reactance surface, which is the largest when the reactance surface becomes perfectly-conducting, is decreased, shifted and blended to the main lobe as λ_b/k varies from 0 to 0.5. Although the field may change considerably in the illuminated region far away from the reactance surface, it is almost the same in the shadow region for different surface impedances (note that this is not the case where the magnetic current line source is located close to the reactive surface which supports a surface wave). When the reactance surface is in the shadow region, the field does not change much as the surface impedance varies; except in the vicinity of the reactance surface, the field tends to decrease more rapidly as λ_b/k increases.

The radiation patterns of an electric current line source illuminating a right-angled wedge are shown in Figs. 17 through 19. The normalized surface admittance, λ_a/k, is chosen to be -1.0, -10 and $-\infty$. The case $\lambda_a/k=-\infty$ corresponds to that of a perfectly-conducting wedge. It is noted that the radiation pattern does not change much as the surface admittance varies.

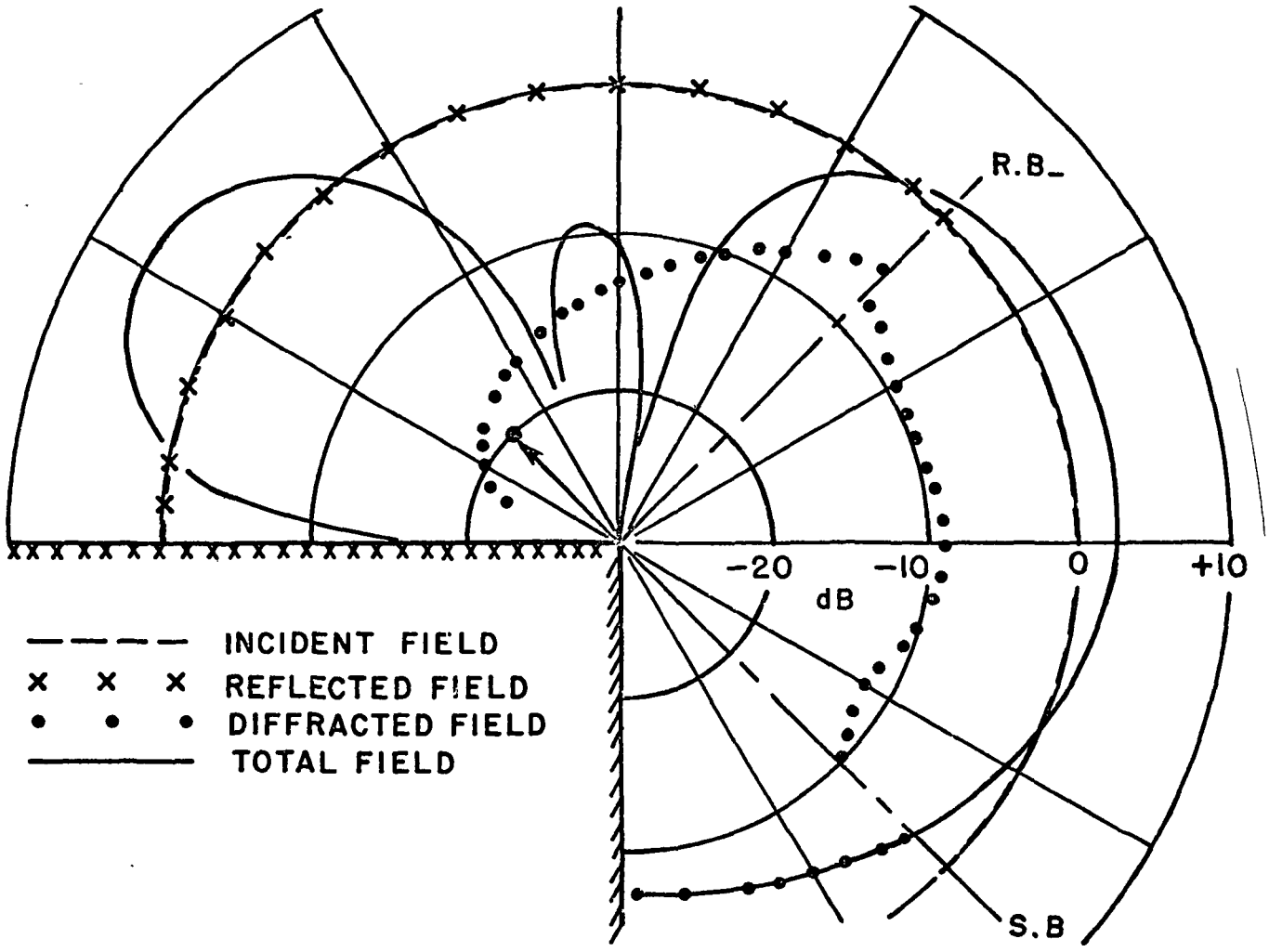

Fig. 13. Radiation pattern of a magnetic line source ($\rho' = 1\lambda$, $\phi' = 45°$, $\lambda_b/k = 0.5$).

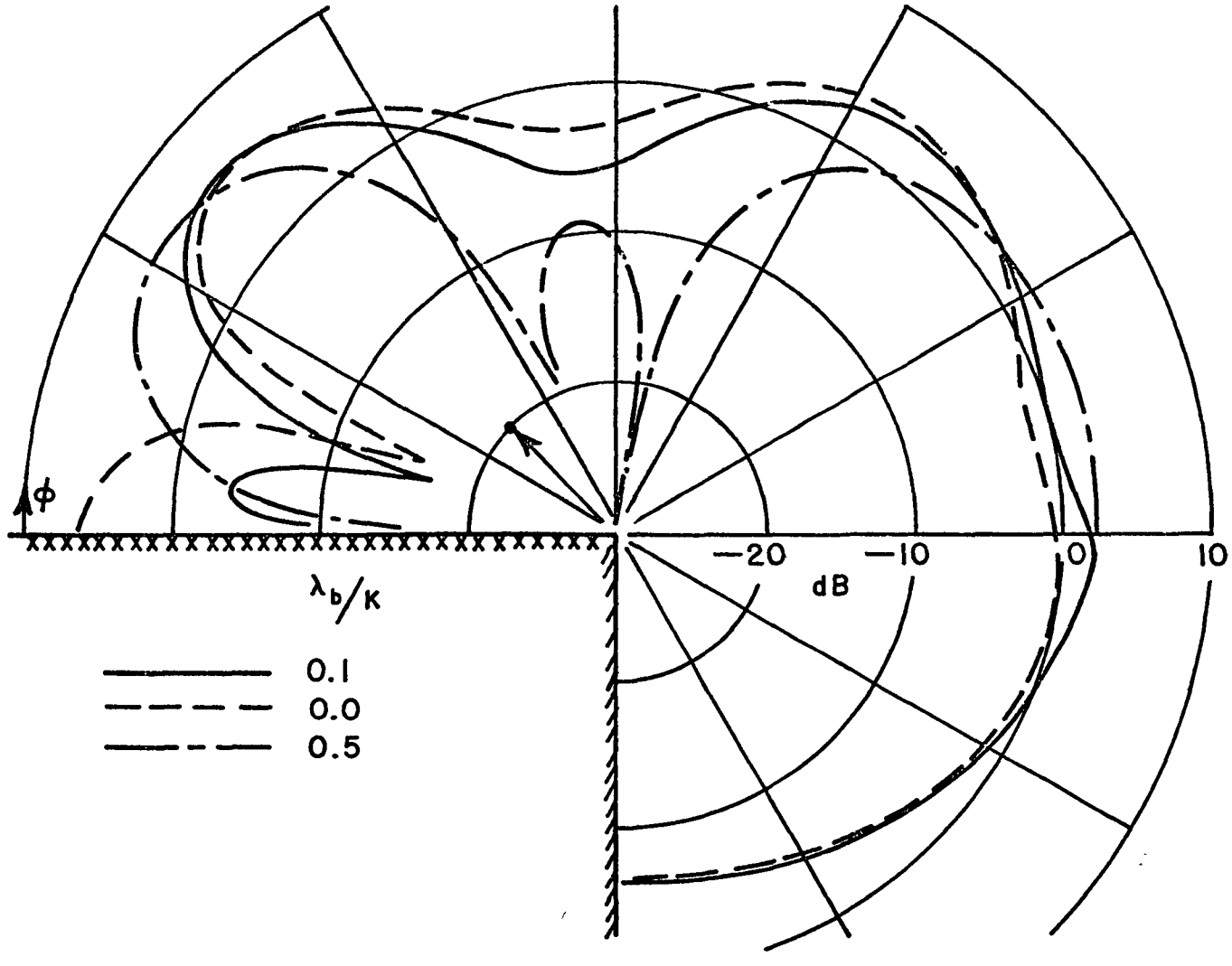

Fig. 14. Radiation pattern of a magnetic line source $\rho' = 1\lambda$, $\phi' = 45°$, λ_b/k: Normalized surface impedance.

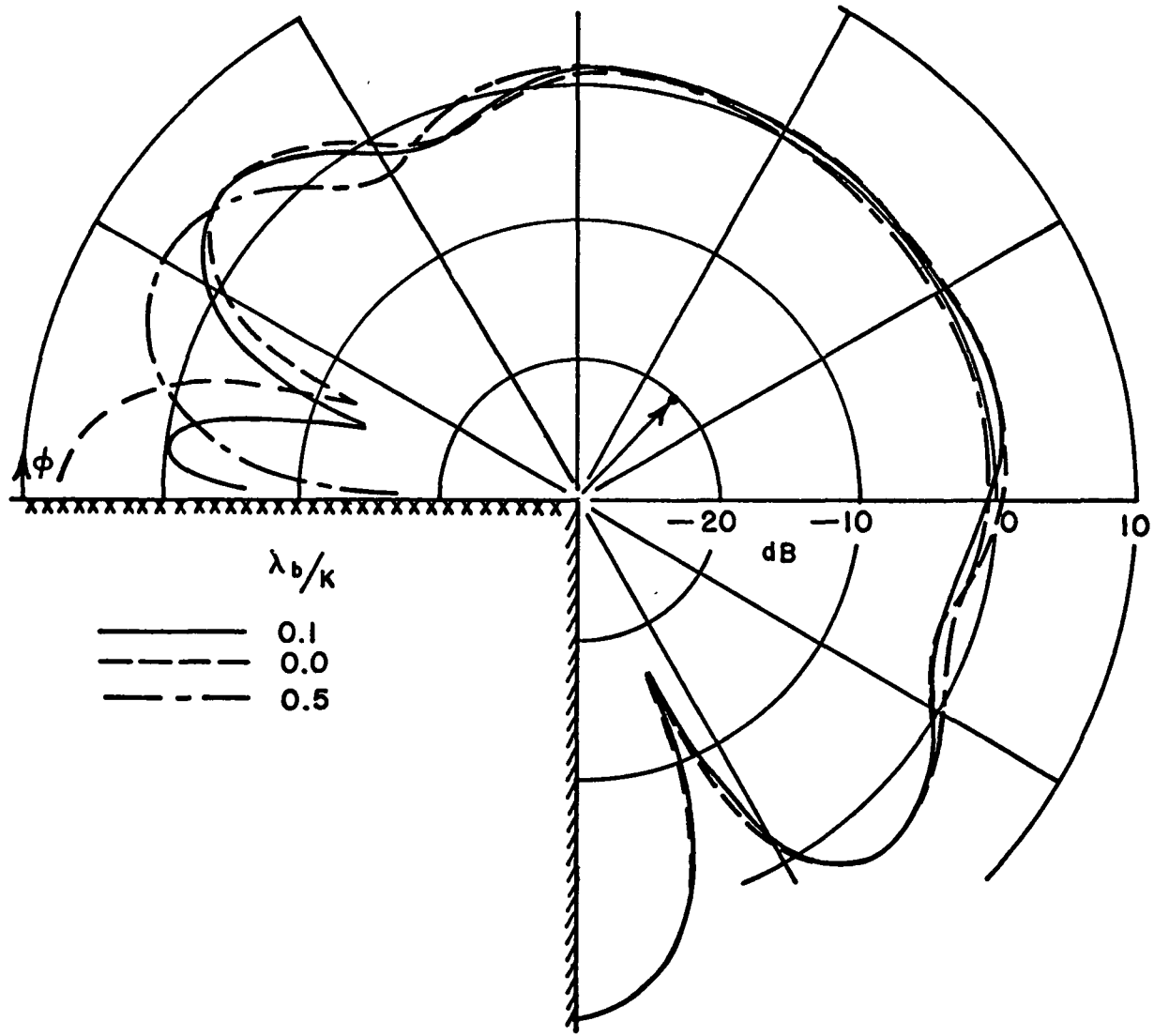

Fig. 15. Radiation pattern of a magnetic line source $\rho' = 1\lambda$, $\phi' = 135°$, λ_b/k: Normalized surface impedance.

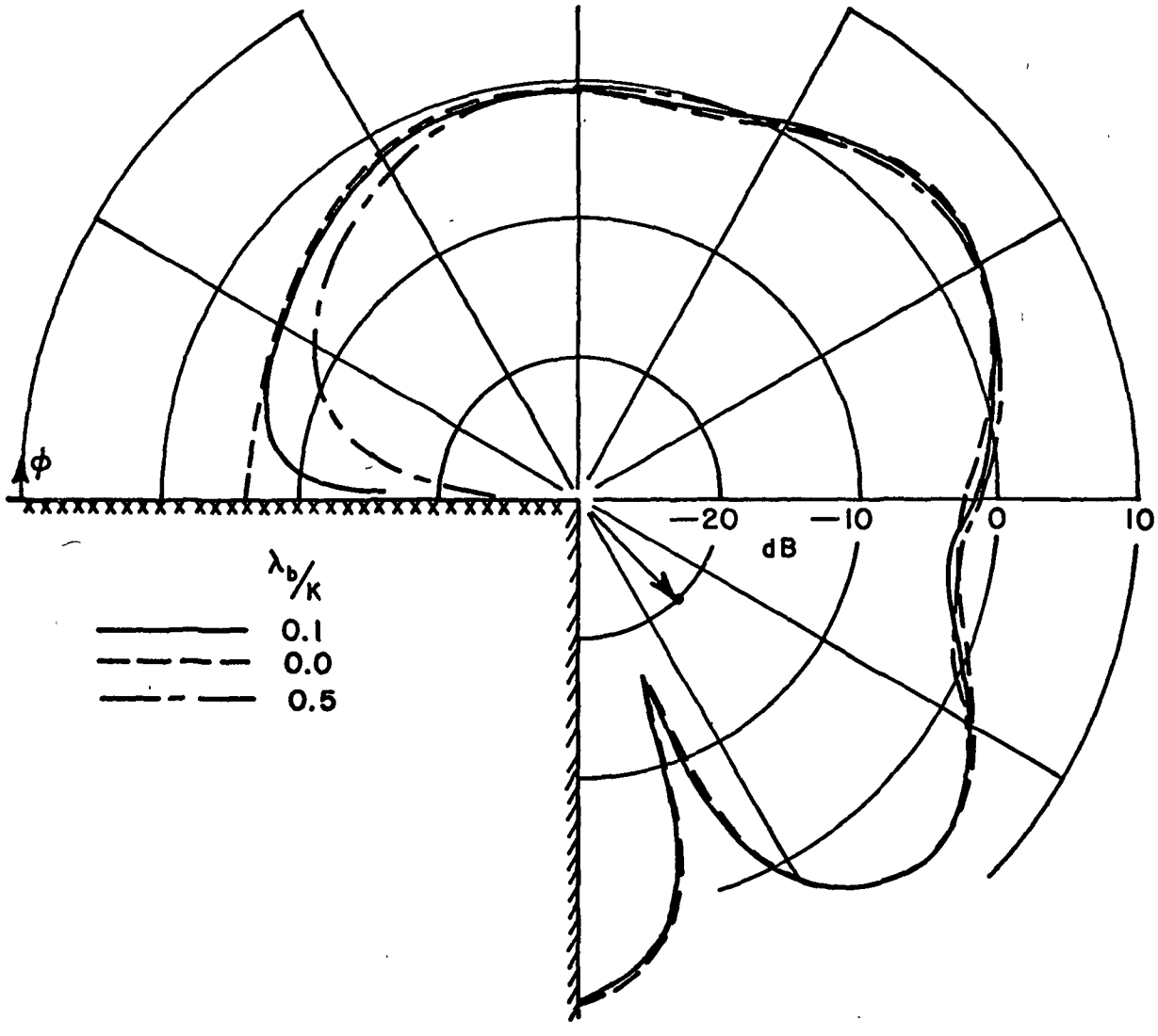

Fig. 16. Radiation pattern of a magnetic line source $\rho' = 1\lambda$, $\phi' = 225°$, λ_b/k: Normalized surface impedance.

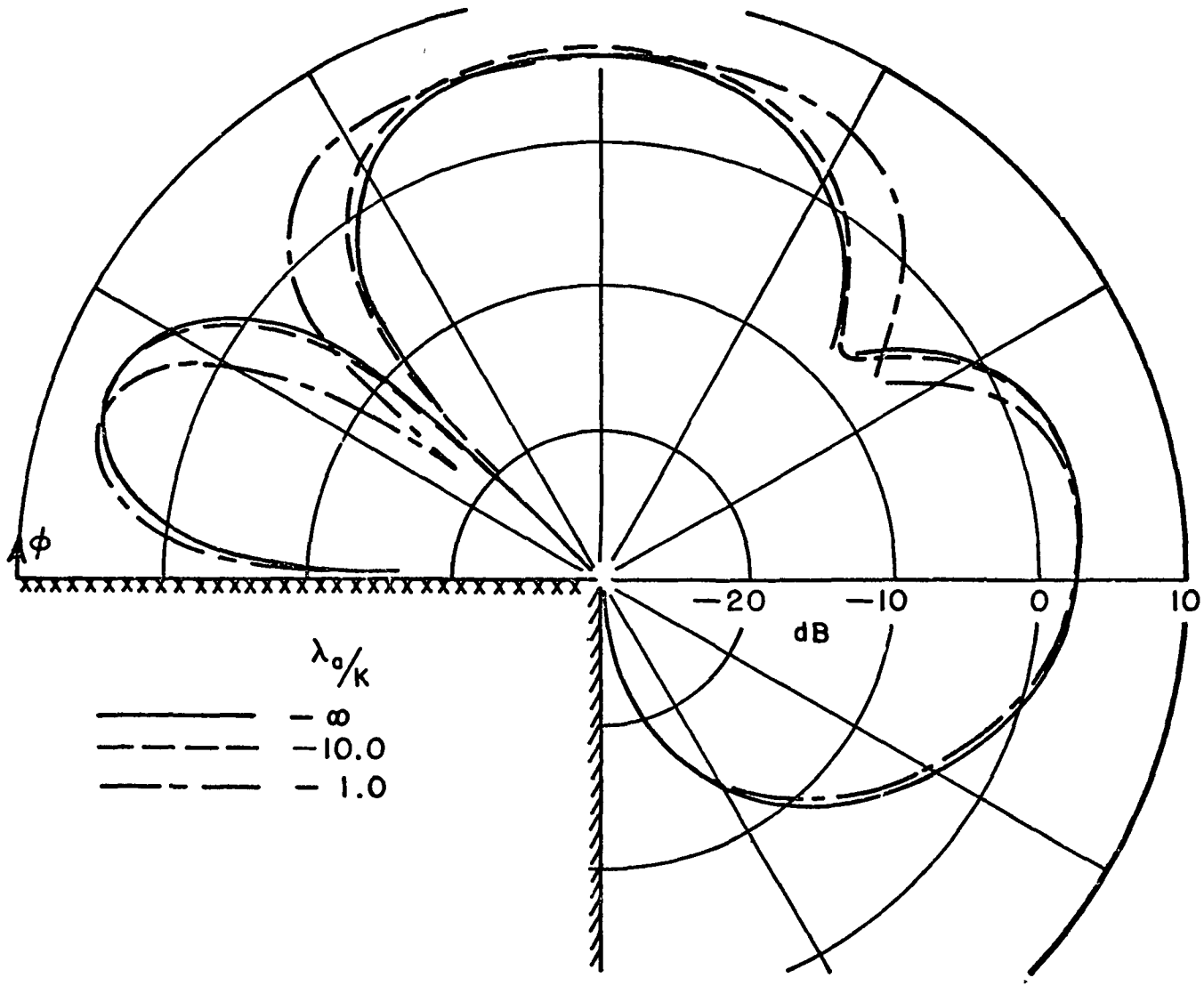

Fig. 17. Radiation pattern of an electric current line source $\rho' = 1\lambda$, $\phi' = 45°$, λ_a/k: Normalized surface admittance.

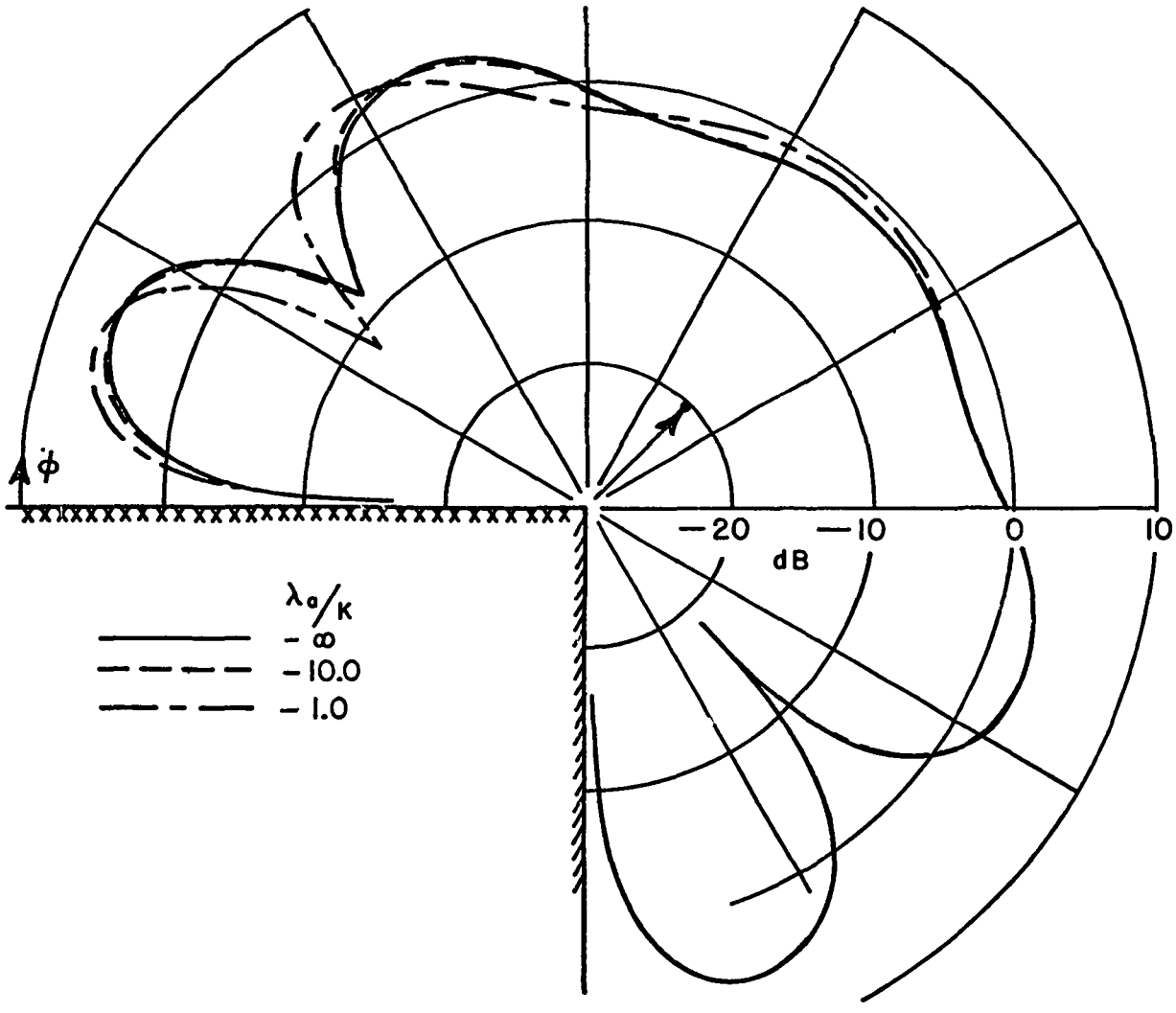

Fig. 18. Radiation pattern of an electric current line source $\rho' = 1\lambda$, $\phi' = 135°$, λ_a/k: Normalized surface admittance.

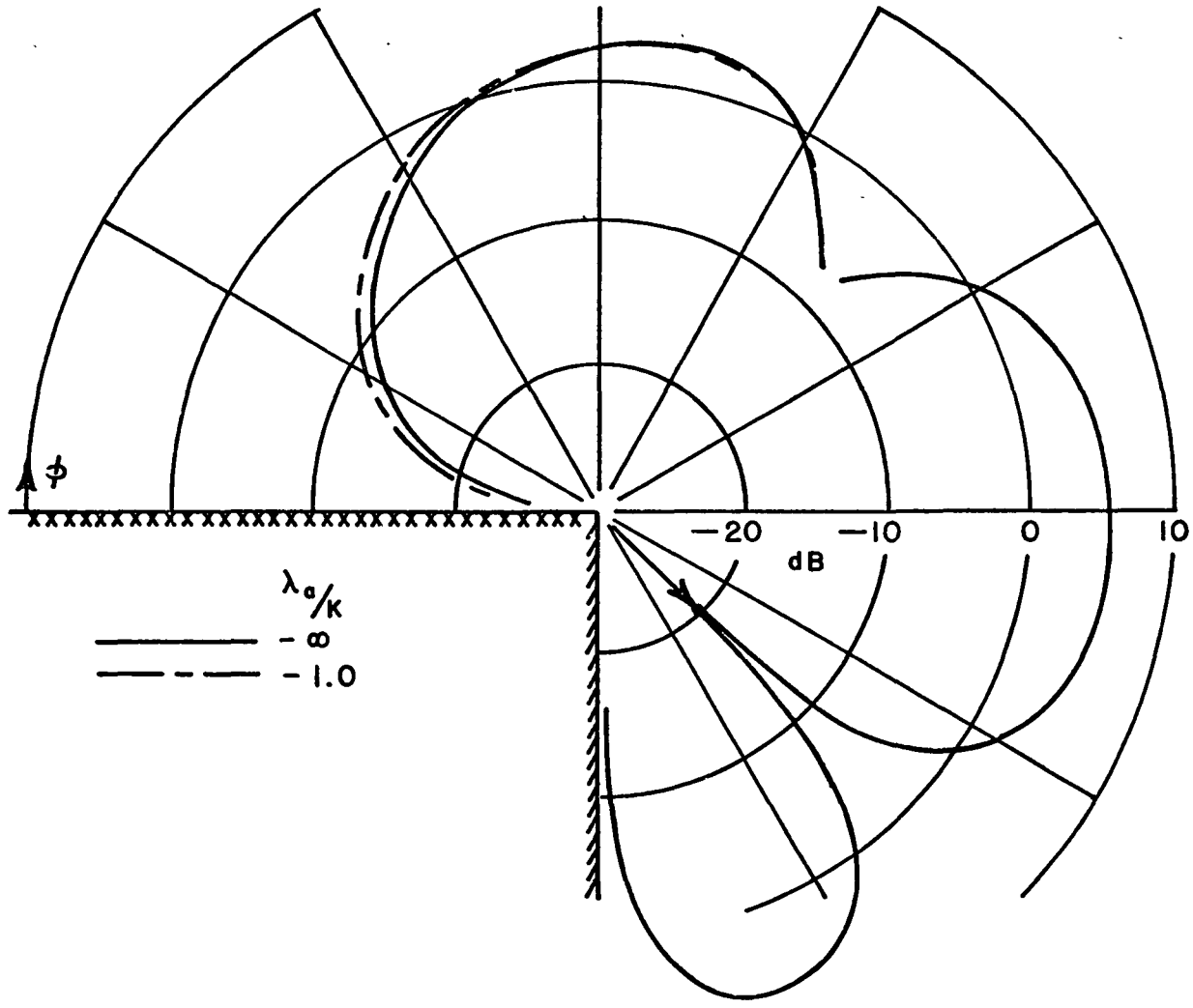

Fig. 19. Radiation pattern of an electric current line source $\rho' = 1\lambda$, $\phi' = 225°$, λ_a/k: Normalized surface admittance.

CHAPTER V
DISCUSSIONS

It has been shown in the last chapter that the solutions for the radiation patterns of a line source in the vicinity of a wedge with a reactive wall are quite good for the analytic models considered. As mentioned earlier, the effect of a coated surface which is covered by a dielectric slab or absorber is approximated by a uniform surface impedance. A uniform surface impedance boundary condition is then prescribed by $\frac{\partial u}{\partial n} + \lambda u = 0$, where $\frac{\partial u}{\partial n}$ is a normal derivative of u at the uniform impedance surface. In an EM problem, the value of λ is given by either

$$\lambda_a = - jk \frac{y_s}{y_o}$$

for a normally incident TE wave or

$$\lambda_b = - jk \frac{z_s}{z_o}$$

for a normally incident TM wave, where y_s and z_s are the surface admittance and the surface impedance of the surface, respectively, k and z_o are the wave number and characteristic impedance of free space and $y_o = \frac{1}{z_o}$. The reflection coefficient can be shown to be

$$R = \frac{jk\sin\phi + \lambda}{jk\sin\phi - \lambda} \quad . \tag{87}$$

In the case of a perfectly absorbing surface, the reflected field is zero. If the surface is perfectly absorbing at $\phi = \frac{\pi}{2}$ which is in the direction normal to the surface,

$$\lambda = - jk. \tag{88}$$

For a dielectric-covered ground plane with the thickness "d", it is easy to show that the reflection coefficient is given by

$$R_{\substack{a\\b}} = \frac{jk\sin\phi + \lambda_{\substack{a\\b}}}{jk\sin\phi - \lambda_{\substack{a\\b}}} \tag{89}$$

where the subscript 'a' denotes the TE case, 'b' denotes the TM case, and

$$\lambda_a = -\zeta \cot\zeta d \tag{90a}$$

$$\lambda_b = \frac{\zeta}{\varepsilon_r} \tan\zeta d, \tag{90b}$$

with

$$\zeta = k\sqrt{\varepsilon_r - \cos^2\phi} \quad . \tag{91}$$

The total field, $U_{\substack{a\\b}}$, satisfies the boundary condition:

$$\left(\frac{\partial}{\partial y} + \lambda_{\substack{a\\b}}\right) U_{\substack{a\\b}} = 0 \tag{92}$$

at the dielectric slab surface. Thus $\lambda_{\substack{a\\b}}$ is a function of the variable ϕ. We assume that if the dielectric slab is not very thick, $\lambda_{\substack{a\\b}}$ can be approximated as a constant which is obtained by solving the root, ζd, of the transcendental equation

$$(\zeta d)\cot\zeta d + \sqrt{(\varepsilon_r - 1)(kd)^2 - (\zeta d)^2} = 0 \tag{93a}$$

for TE case and

$$(\zeta d)\tan\zeta d - \varepsilon_r\sqrt{(\varepsilon_r - 1)(kd)^2 - (\zeta d)^2} = 0 \tag{93b}$$

for TM case. The root of the above equations corresponds to the surface wave mode if the dielectric-covered surface sustains a surface wave. It has been found numerically that the diffracted field is not very sensitive to the variation of the approximate surface impedance, but as far as the reflected field is concerned, this is not the case. Figure 20 shows the radiation pattern of an infinite, dielectric-covered ground plane illuminated by an electric current line source. The total radiation field is the sum of the incident field and the reflected field. In Fig. 20 it is apparent that there is a great deal of discrepancy between the exact radiation field and those computed by using the surface impedance model. This analysis, of course, shows an error in the reflected geometric field. A proportionate error will exist in the reflected diffracted field, i.e., the diffracted field associated with the reflection boundary, if the edge lies in the range $50° < \phi^i < 130°$ for this particular geometry. Outside this range, the reflected geometric field should be reasonably accurate. The incident geometric and the incident diffracted will be little changed by the presence of the reactive wall. Thus, we suggest that when the dielectric-covered surface is in this illuminated region, the exact reflection coefficient in Eq. (89) is used instead of the approximate reflection coefficient obtained from the surface impedance model for the geometrical optics field. This would lead to a discontinuity of the order of 10 dB. The value of λ should be taken from Eqs. (90a) or (90b) at $\phi = \phi^i$ in order to make the total field continuous across the reflection boundary. When the dielectric slab is very thin, it can be shown that

$$\lambda_a \sim -\frac{1}{d}, \tag{94a}$$

and

$$\lambda_b \sim \frac{\varepsilon_r - 1}{\varepsilon_r} k^2 d. \tag{94b}$$

Thus the uniform surface impedance is a good approximation for this case.

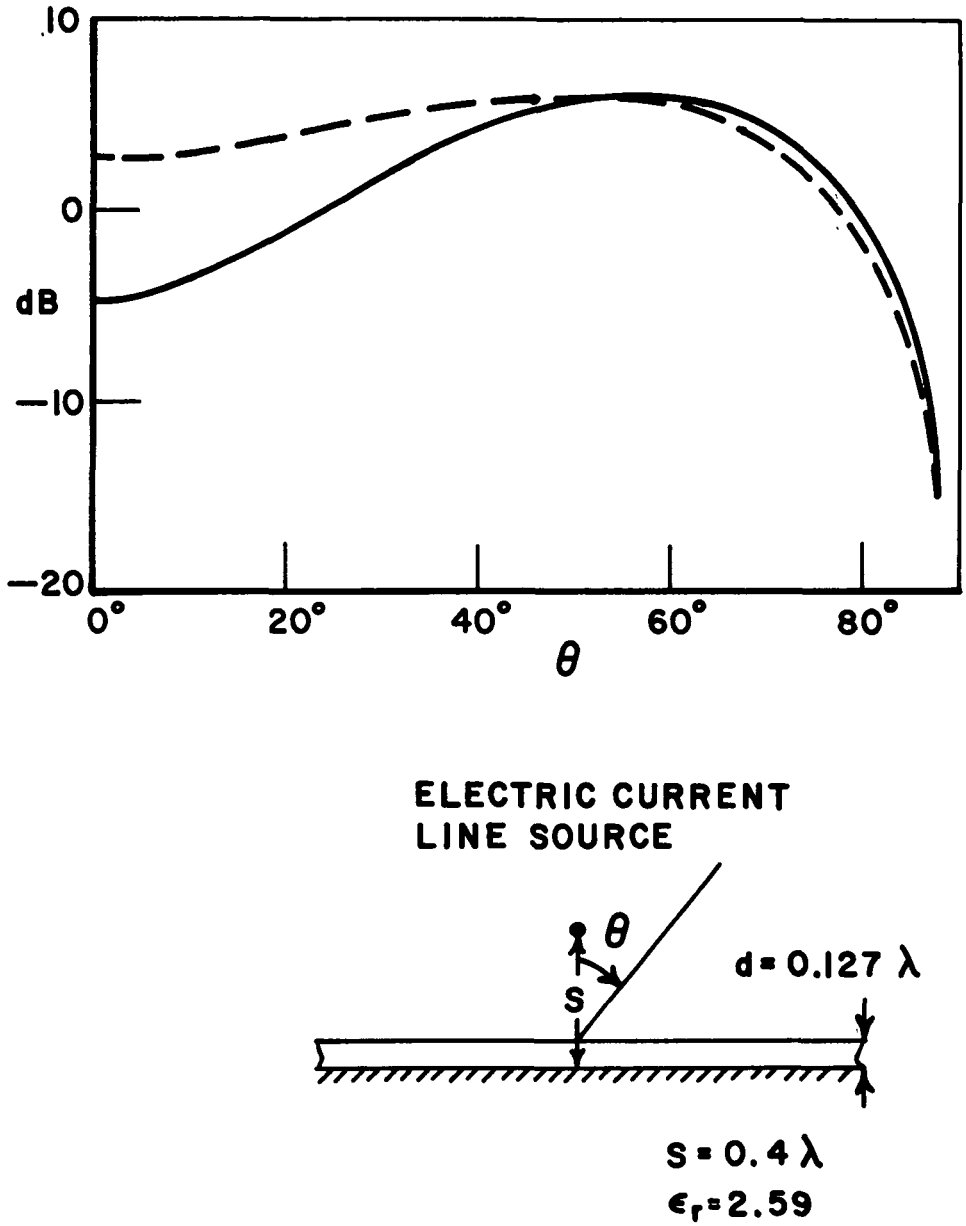

Fig. 20. Radiation pattern of an infinite dielectric-covered ground plane (d = 0.127λ, ε_r = 2.59) illuminated by an electric current line source (S = 0.4λ).

The total solution of a differential equation is the sum of particular solution and homogeneous solution. The homogeneous solution of Eq. (6) is $e^{-\lambda y}f(x)$. When $\lambda>0$, this solution is bounded and therefore exists in the domain of interest, which is recognized as a surface wave. Unfortunately our method fails to find the amplitude of this surface wave.

The strength of the surface wave was obtained for TM plane wave illumination and a magnetic current line source located on the tip of the wedge by Karp and Karal[7,9]. The method they used is that after the functional transformation, the homogeneous solution of the transformed differential equation is chosen to be

$$C_1 H_{\frac{1}{3}}^{(2)}(k\rho) \cos \frac{\phi}{3}$$

instead of that given by H (see Eq. (15)). The function

$$C_1 H_{\frac{1}{3}}^{(2)}(k\rho) \cos \frac{\phi}{3}$$

does not satisfy all the conditions of the problem, since, following the inverse transformation its x derivative is discontinuous at the positive y axis. Thus the function $C_2 e^{-\lambda y}$ is introduced in the total field in the region $x\geq 0$, $y\geq 0$ to make it possible to satisfy the continuity condition involving the x derivative of U. C_1 and C_2 are then obtained. For the case of a magnetic (or electric) current line source located far from the edge of the wedge, the strength of the surface wave can be obtained in the same way. However, two cases should be considered separately: $\phi' < \frac{\pi}{2}$ and $\phi' > \frac{\pi}{2}$. In the former case, the line current source excites a surface wave which propagates toward and away from the edge. The strength of excitation of the surface wave is assumed to be the same as those due to a uniform line current source located above the same impedance

surface of infinite extent. The justification of this assumption is that the line source is far from the edge, i.e., the exciting device is in the far zone of the scattering from the termination which is, in our problem, the edge of the wedge. The surface wave field is well established and propagates along the impedance surface before it reaches the edge. Thus in matching the continuous condition at the line $\{x=0, y>0\}$, this excited incident surface wave should be included in the total field. However, in the latter case, there is no such incident surface wave included.

Several approximations have been made in deriving Eq. (90). According to the geometrical theory of diffraction, it has been assumed that the high-frequency diffracted field propagated along its ray path perpendicular to the diffracted electric and magnetic fields in the same way as the geometrical optics field. This approximation does not introduce a large error if both the source point and the field point are far from the edge. Second, in deriving Eq. (90), it has been assumed that kL is large. However, based on the extensive numerical study of asymptotic solutions of this type presented in References [5] and [20], it would appear that this approximation generally introduces serious error only when $kL < 1$.

The preceding discussion has been restricted to the diffraction by wedges with straight edges; however the geometrical theory of diffraction can be used to treat the diffraction from curved edges[20]. The diffracted ray paths are determined by the generalized Fermat's principle for edge diffraction, and the conservation of power flow in the resulting astigmatic bundle of rays, see Fig. 21, leads to the general spatial attenuation factor

$$A(s) = \sqrt{\frac{\rho_c}{s(\rho_c+s)}} \tag{95}$$

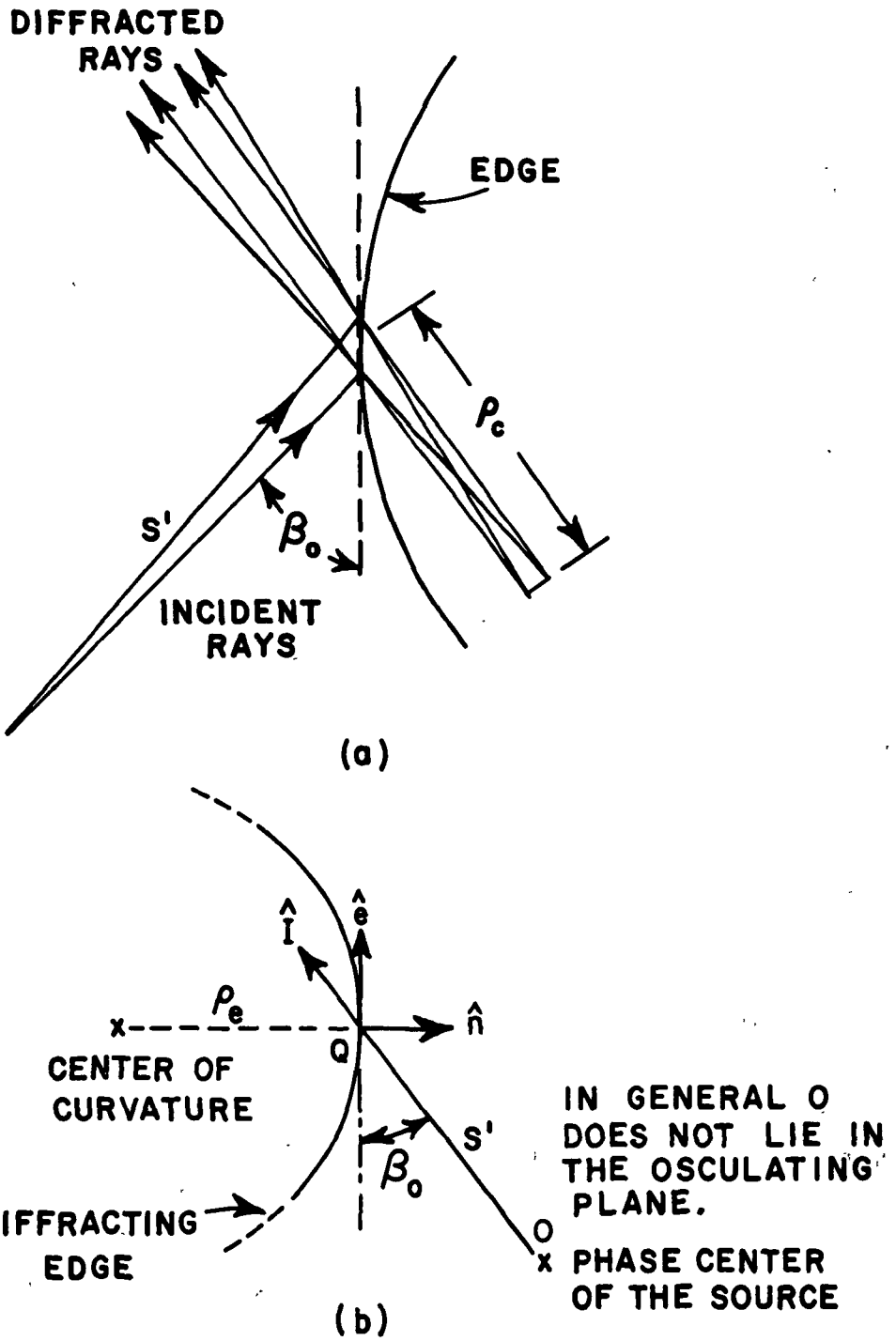

Fig. 21. Diffraction at a curved edge.

where the caustic distance ρ_c shown in Fig. 21 is given by

$$\frac{1}{\rho_c} = \frac{1}{s'} - \frac{\hat{n} \cdot (\hat{I} - \hat{s})}{\rho_e \sin^2\beta_o} \tag{96}$$

for spherical wave illumination of the edge[14]. In the equation above

ρ_e is the radius of curvature of the edge

$\hat{n}$ is the unit vector normal to the edge

$\hat{I}, \hat{s}$ are unit vectors in the directions of incident and diffraction, respectively,

β_o is the angle between $\hat{I}$, $\hat{e}$, the tangent to the edge at the point of diffraction, see Fig. 22.

The expression for A(s) given in Eq. (95) will reduce to that given in Eq. (75) if ρ_e is set equal to infinity for the straight edge; furthermore, for plane and cylindrical wave illumination of the straight edge, $\rho_c = \infty$.

The diffraction coefficient is assumed to be independent of ρ_e to a first approximation; this is a reasonable assumption because it is independent of the curvature of the incident wavefront to this approximation, as has been demonstrated in Chapters II and III. Furthermore, the validity of this assumption has been confirmed in numerical applications of the geometrical theory of diffraction to structures with curved edges of a perfectly-conducting wedge[14,20]. Thus, in accordance with the postulates of the geometrical theory of diffraction, Eq. (74) becomes

$$\vec{E}^d(s) = \vec{E}^i(Q_E) \cdot \bar{\bar{D}}_E(s,I) \sqrt{\frac{\rho_c}{s(\rho_c+s)}}\ e^{-jks} \tag{97}$$

where $\bar{\bar{D}}_E$ is identical to Eq. (76) with $\beta_o = \frac{\pi}{2}$. Alternatively, if the incident and diffracted fields are decomposed into components parallel and perpendicular to the plane of incidence and diffraction, respectively, we can write Eq. (97) in terms of matrix notation as

$$(98) \qquad \begin{bmatrix} E_{\parallel}^{d} \\ E_{\perp}^{d} \end{bmatrix} = \begin{bmatrix} D_a & 0 \\ 0 & D_b \end{bmatrix} \begin{bmatrix} E_{\parallel}^{i} \\ E_{\perp}^{i} \end{bmatrix} \sqrt{\frac{\rho_c}{s(\rho_c+s)}}\, e^{-jks}.$$

By introducing the ray-fixed coordinate system the polarization effects of high-frequency scattering can be greatly simplified, whether this involves the reflection from a smooth curved surface, the diffraction from an edge, or the diffraction from a smooth curved surface. Specifically, the polarization of the scattered field can be related to the polarization of the incident field by a 2x2 diagonal matrix.

Several important steps used to solve this boundary valued problem are briefly described in the following to show the merit of the method employed. The mixed boundary condition of a wave equation is transformed to a simple homogeneous one by a functional transformation. In general, the transformed wave equation becomes complicated at the expense of the simplification of the boundary condition. By using the fact that the operator, $L = \frac{\partial}{\partial y} + \lambda$, of the functional transformation and $(\nabla^2 + k^2)$ commute and $\frac{\partial}{\partial y}\delta(y-y') = -\frac{\partial}{\partial y'}\delta(y-y')$, the solution of the transformed wave equation can be related to some special Green's functions which satisfy the simple homogeneous boundary conditions. Although the technique is applied for the right-angled wedge in this report, Karp[10] pointed out that it could also be used to simplify the boundary value problem for some special angular spaces. Currently, this method is extended to treat an arbitrary-angled wedge with one of its surfaces satisfying a uniform

surface impedance boundary condition while the other, a perfectly-conducting surface, satisfying Dirichlet boundary condition. The far zone approximation at the perfectly-conducting surface is made after the functional transformation so that Dirichlet boundary condition remains unchanged. Thus the boundary conditions of the transformed wave equation still become homogeneous. The method can also be employed for a right-angled wedge with two uniform impedance surface walls. Recently, the diffraction of a two-part plane by a plane wave illumination is already pursued by the Wiener-Hopf technique; one part of its surface satisfying a uniform surface impedance boundary condition while the other being perfectly-conducting. The transformation technique fails for this case since the boundary conditions of the transformed wave equation can not be simplified by using the functional transformation.

In summary, Maxwell's equations can be solved exactly for few problems with appropriate boundary conditions. Hence approximations have to be made to obtain solutions to useful problems. High-frequency asymptotic approximation is used to solve the diffraction problem. Mathematically speaking, by making a transformation which simplifies the boundary condition and employing the modified Pauli-Clemmow method of steepest descent, the diffraction coefficient has been found for the right-angled wedge with one wedge face satisfying a uniform impedance boundary condition. The introduction of a ray-fixed coordinate system yields a compact, dyadic diffraction coefficient for EM waves illumination. This diffraction coefficient is also valid in the transition regions of the shadow and reflection boundaries for a variety of edge illuminations. The geometrical theory of diffraction is used to extend the solution to more general cases, such as the curved edge. The diffraction coefficient is composed of trigonometric functions and Fresnel integrals which are easy to compute.

APPENDIX I
AN ASYMPTOTIC APPROXIMATION FOR SCALAR WEDGE DIFFRACTION VIA THE MODIFIED STEEPEST DESCENT METHOD

A. Cylindrical Wave Illumination

Let us consider a scalar field U_b^a which satisfies the wave equation

$$(\nabla_t^2 + k^2)\, U_b^a = -\,\delta(x-x')\,\delta(y-y') \tag{A-1}$$

with the boundary conditions

$$\left(\frac{\partial}{\partial y} + \lambda_b^a\right) U_b^a = 0 \;; \qquad \phi = 0. \tag{A-2}$$

$$\begin{cases} U_a = 0 \\ \dfrac{\partial U_b}{\partial \phi} = 0 \end{cases} \;; \qquad \phi = n\pi \tag{A-3}$$

and which also satisfies the Sommerfeld radiation condition and the Meixner edge condition and n=1.5. In Eq. (20) the far-zone form of U_b^a was shown to be

$$U_b^a \sim \frac{\left[(C-1)\frac{\partial}{\partial y'} + \lambda_b^a\right] G - jkC\sin\phi W}{-jk\sin\phi + \lambda_b^a} \tag{A-4}$$

where G and W are two known special Green's functions given in Eqs. (11a), (11b), (13a) and (13b), and C is a constant to be determined. The geometrical configuration is depicted in Fig. 2.

An integral representation for the product, $J_{\nu_m}(k\rho')H^{(2)}_{\nu_m}(k\rho)$ is Reference [16]

$$(A\text{-}5) \qquad J_{\nu_m}(k\rho')H^{(2)}_{\nu_m}(k\rho) = -\frac{1}{\pi j}\int_0^{C-j\infty} e^{\frac{1}{2}[t-k^2(\rho^2+\rho'^2)t^{-1}]} I_{\nu_m}\left(\frac{k^2\rho\rho'}{t}\right)\frac{dt}{t},$$

where $C > 0$, $\nu_m > -1$ and $|\rho'| < |\rho|$. $I_{\nu_m}\left(\frac{k^2\rho\rho'}{t}\right)$ represents the modified cylindrical Bessel function of the first kind. The integral representation for $I_{\nu_m}\left(\frac{k^2\rho\rho'}{t}\right)$ is given by Reference [16]

$$(A\text{-}6) \qquad I_{\nu_m}\left(\frac{k^2\rho\rho'}{t}\right) = -\frac{1}{2\pi}\int_{\gamma+j\infty}^{\gamma'+j\infty} e^{\frac{k^2\rho\rho'}{t}\cos\xi + j\nu_m\xi}\, d\xi$$

where $-\pi < \gamma' < 0$ and $\pi < \gamma < 2\pi$. Thus

$$(A\text{-}7a) \qquad I_{\nu_m}\left(\frac{k^2\rho\rho'}{t}\right) = -\frac{1}{2\pi}\int_L e^{\frac{k^2\rho\rho'}{t}\cos\xi + j\nu_m\xi}\, d\xi$$

or

$$(A\text{-}7b) \qquad I_{\nu_m}\left(\frac{k^2\rho\rho'}{t}\right) = -\frac{1}{2\pi}\int_{L'} e^{\frac{k^2\rho\rho'}{t}\cos\xi - j\nu_m\xi}\, d\xi .$$

The contours L and L' are indicated in Fig. 22. Let $\beta^{\pm} = \phi \pm \phi$, then Eqs. (11b) and (13a) can be written as

$$(A\text{-}8) \qquad G_b = g(\bar{\rho},\bar{\rho}';\beta^-) - g(\bar{\rho},\bar{\rho}';\beta^+)$$

and

$$(A\text{-}9) \qquad W_a = g(\bar{\rho},\bar{\rho}';\beta^-) + g(\bar{\rho},\bar{\rho}';\beta^+)$$

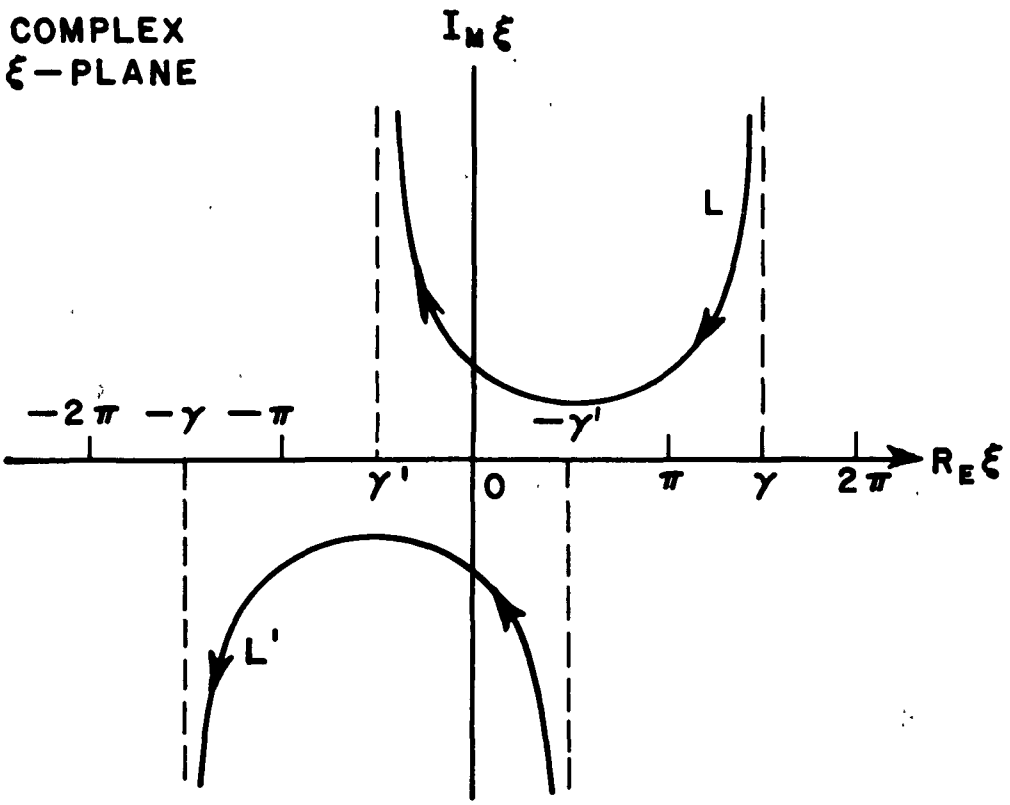

Fig. 22. The L and L' contours for the integral representation of $I_{\frac{m}{n}}(\frac{k^2\rho\rho'}{t})$ in the complex ξ-plane.

where

$$(A\text{-}10) \qquad g(\bar{\rho},\bar{\rho}';\beta) = -\frac{j}{4n}\sum_{m=0}^{\infty} J_{\frac{2m+1}{2n}}(k\rho')H^{(2)}_{\frac{2m+1}{2n}}(k\rho)\left(e^{j\frac{2m+1}{2n}\beta} + e^{-j\frac{2m+1}{2n}\beta}\right)$$

Note that $\cos\frac{2m+1}{2n}$ is replaced by $\frac{1}{2}\left(e^{j\frac{2m+1}{2n}} + e^{-j\frac{2m+1}{2n}}\right)$.

Substituting Eqs. (A-6) and (A-7) into (A-10), we obtain

$$(A\text{-}11)\qquad g(\bar{\rho},\bar{\rho};\beta) = -\frac{1}{8\pi^2 n}\int_0^{C-j\infty} e^{\frac{1}{2}[t-k^2(\rho^2+\rho'^2)t^{-1}]} \times$$

$$\times\left\{\int_L e^{\frac{k^2\rho\rho'}{t}\cos\xi}\sum_{m=0}^{\infty} e^{j\frac{2m+1}{2n}(\xi+\beta)}\,d\xi + \right.$$

$$\left. + \int_{L'} e^{\frac{k^2\rho\rho'}{t}\cos\xi}\sum_{m=0}^{\infty} e^{-j\frac{2m+1}{2n}(\xi+\beta)}\,d\xi\right\}\frac{dt}{t}\,.$$

By noting that

$$(A\text{-}12a)\qquad \sum_{m=0}^{\infty} e^{j\frac{m}{n}(\xi+\beta)} = -\frac{1}{2j}\cot\left(\frac{\xi+\beta}{2n}\right) + \frac{1}{2},$$

and

$$(A\text{-}12b)\qquad \sum_{m=0}^{\infty} e^{-j\frac{m}{n}(\xi+\beta)} = \frac{1}{2j}\cot\left(\frac{\xi+\beta}{2n}\right) + \frac{1}{2}$$

$$(A\text{-}13a)\qquad \sum_{m=0}^{\infty} e^{j\frac{2m+1}{2n}(\xi+\beta)} = -\frac{1}{2j}\,\frac{\cos^2\left(\frac{\xi+\beta}{2n}\right)}{\sin\left(\frac{\xi+\beta}{2n}\right)} + \sin\left(\frac{\xi+\beta}{2n}\right),$$

$$(A\text{-}13b)\qquad \sum_{m=0}^{\infty} e^{-j\frac{2m+1}{2n}(\xi+\beta)} = \frac{1}{2j}\,\frac{\cos^2\left(\frac{\xi+\beta}{2n}\right)}{\sin\left(\frac{\xi+\beta}{2n}\right)} + \sin\left(\frac{\xi+\beta}{2n}\right)$$

and Reference [16]

$$(A\text{-}14)\qquad -\frac{1}{2}\int_{C-j\infty}^{0} e^{\frac{t}{2}-\frac{z^2}{2t}}\,\frac{dt}{t} = K_0(jZ).$$

Equation (A-11) can be simplified as

$$(A\text{-}15) \qquad g(\bar{\rho},\bar{\rho};\beta) = \frac{1}{8\pi^2 nj} \int_{L-L'} d\xi \left[\frac{\cos^2(\frac{\xi+\beta}{2n})}{\sin(\frac{\xi+\beta}{2n})} + \sin(\frac{\xi+\beta}{2n}) \right] K_0(jZ(\xi))$$

where $K_0(jZ)$ is the modified cylindrical Bessel function of the second kind, of order zero and argument jZ, and $Z(\xi) = k\sqrt{\rho^2+\rho'^2 - 2\rho\rho' \cos\xi}$. We are interested in solutions for which $Z(\xi)$ is sufficiently large which will be justified later.

If $|Z(\xi)|$ is large, $K_0(jZ(\xi))$ can be replaced by its large argument approximation

$$(A\text{-}16) \qquad K_0(jZ(\xi)) \sim \sqrt{\frac{\pi}{2jZ(\xi)}}\, e^{-jZ(\xi)} \quad .$$

In the asymptotic solution described later, it will be seen that $\rho^2+\rho'^2-2\rho\rho\cos\xi >> 0$ in the neighborhood of the saddle points, therefore

$$(A\text{-}17) \qquad e^{-jkZ(\xi)} = e^{-jk\sqrt{(\rho+\rho')^2-2\rho\rho'(1+\cos\xi)}}$$

$$\sim e^{-jk(\rho+\rho')[1 - \frac{\rho\rho'}{(\rho+\rho')^2}(1+\cos\xi)]} \quad .$$

Thus

$$(A\text{-}18) \qquad g(\bar{\rho},\bar{\rho}';\beta) \sim e^{-jk(\rho+\rho')} \int_{L-L'} \sqrt{\frac{2}{j\pi k(\rho^2+\rho'^2-2\rho\rho'\cos\xi)^{1/2}}}\ x$$

$$F_1(\xi,\beta)\, e^{\kappa f(\xi)}\, d\xi$$

where

(A-19a) $$F_1(\xi,\beta) = \frac{1}{4\pi nj}\left[\frac{\cos^2(\frac{\xi+\beta}{2n})}{\sin(\frac{\xi+\beta}{2n})} + \sin(\frac{\xi+\beta}{2n})\right]$$

(A-19b) $$f(\xi) = j(1 + \cos\xi)$$

and

(A-19c) $$\kappa = \frac{k\rho\rho'}{\rho+\rho'} \quad .$$

Therefore the integral in Eq. (A-18) is in the proper form to be evaluated by the method of steepest descent for a large parameter. The saddle points of $f(\xi)$ occur at

$$\frac{d}{d\xi} f(\xi)\Big|_{\xi=\xi_s} = 0 \ ;$$

but only $\xi_s = \pm \pi$ are considered because the steepest descent paths through $\xi_s = \pm \pi$ allow us to close the (L-L') contour. It is clear that in the neighborhood of these saddle points the inequality in $\rho^2+\rho'^2 >> 2\rho\rho'\cos$ is satisfied, which justifies the approximation in Eq. (A-16). Figure 23 shows the locations of the steepest descent paths through the saddle points at $\xi_s = \pm \pi$. Therefore

(A-20)

$$e^{-jk(\rho+\rho')} \int_{L-L'} d\xi \, F_1(\xi,\beta) \sqrt{\frac{2}{j\pi k(\rho^2+\rho'^2-2\rho\rho'\cos\xi)^{1/2}}}\, e^{\kappa f(\xi)}$$

$$= - e^{-jk(\rho+\rho')}\left[\int_{SDP(\pi)} + \int_{SDP(-\pi)} d\xi \, F_1(\xi,\beta) \sqrt{\frac{2}{j\pi k(\rho^2+\rho'^2-2\rho\rho'\cos\xi)^{1/2}}}\, e^{\kappa f(\xi)}\right]$$

$$+ \quad 2\pi j \Sigma \left[\begin{array}{l}\text{The residues of the integrand enclosed} \\ \text{by L-L' and SDP } (\pm\pi)\end{array}\right]$$

+ Branch cut contributions, if any.

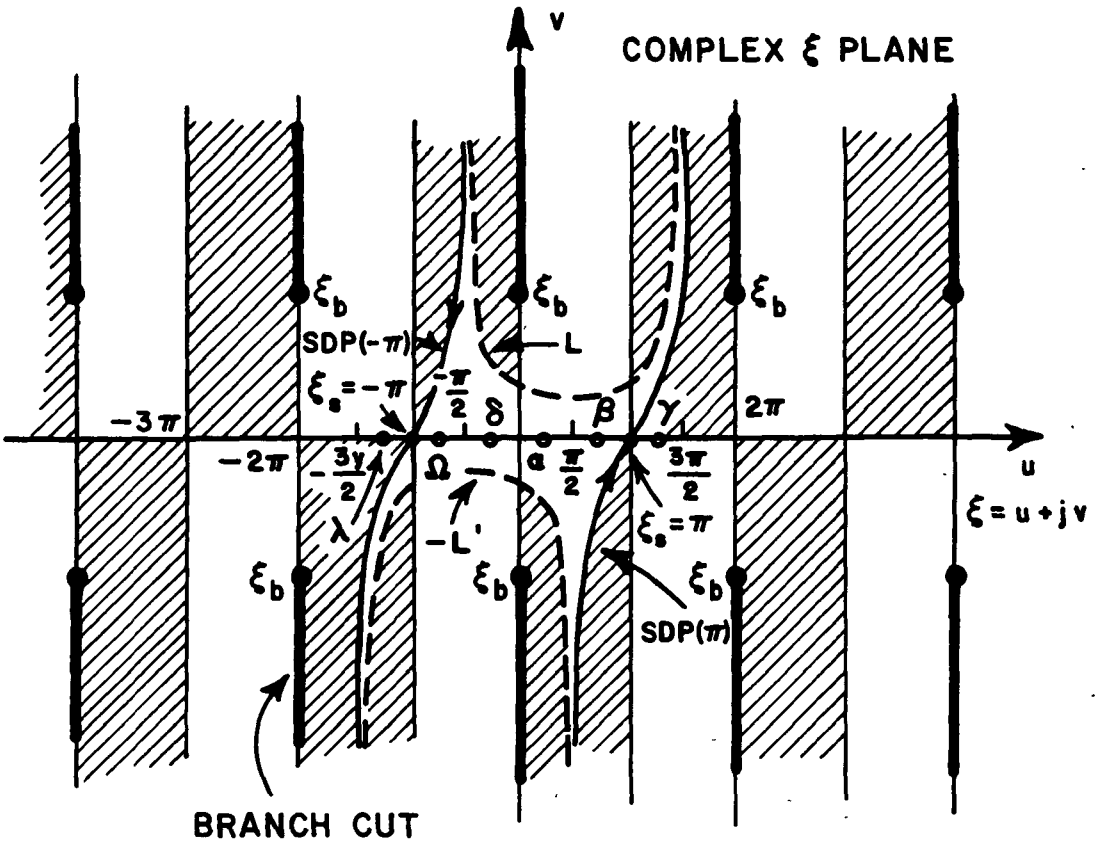

Fig. 23. Steepest descent paths (SDP $\pm \pi$) and the complex ξ plane topology.

The pole singularities occur at

$$\xi_p = -\beta + 2nN\pi \ , \quad N = 0, \pm 1, \pm 2, \cdots \ .$$

The residues corresponding to ξ_p are evaluated only for those $|\xi_p| \leq \pi$. Let the poles contribution to g be denoted by g^p, thus

(A-21)

$$g^p(\bar{\rho},\bar{\rho}';\beta) = \sqrt{\frac{2}{j\pi k(\rho^2+\rho'^2-2\rho\rho'\cos\xi_p)^{1/2}}}\, e^{-jk(\rho^2+\rho'^2-2\rho\rho'\cos\xi_p)^{1/2}} \cos N\pi \times$$

$$\times H[\pi-|\beta+2nN\pi|]$$

where

$$(A\text{-}22) \qquad H(t) = \begin{cases} 0 , & t < 0 \\ \frac{1}{2} , & t = 0 \\ 1 , & t > 1 \end{cases} .$$

The saddle points contribution to g, which is denoted by g^d, is derived via the modified steepest descent method[20], where the pole singularity close to the saddle point is taken into consideration. Thus g^d can be written as

$$(A\text{-}23) \qquad g^d(\bar{\rho},\bar{\rho}';\beta) \sim \left[-\frac{j}{4}\sqrt{\frac{2j}{\pi k\rho'}}\, e^{-jk\rho'} \right] d_g \frac{e^{-jk\rho}}{\sqrt{\rho}}$$

where

$$(A\text{-}24) \qquad d_g(\beta) = -\frac{e^{-j\frac{\pi}{4}}}{2n\sqrt{2\pi k}} \left\{ \left[\sin\left(\frac{\pi+\beta}{2n}\right) + \sin\left(\frac{\pi-\beta}{2n}\right) \right] + \right.$$
$$\left. + \frac{\cos^2\left(\frac{\pi+\beta}{2n}\right)}{\sin\left(\frac{\pi+\beta}{2n}\right)} F[\kappa a^+(\beta)] + \frac{\cos^2\left(\frac{\pi-\beta}{2n}\right)}{\sin\left(\frac{\pi-\beta}{2n}\right)} F[\kappa a^-(\beta)] \right\}$$

with

$$(A\text{-}25) \qquad F[\kappa a^{\pm}(\beta)] = 2j\sqrt{\kappa a^{\pm}(\beta)}\, e^{j\kappa a^{\pm}(\beta)} \int_{\sqrt{\kappa a^{\pm}(\beta)}}^{\infty} e^{-jt^2}\, dt,$$

where the positive branch of the square root is taken,

$$a^{\pm}(\beta) = [1 + \cos(-\beta + 2nN^{\pm}\pi)],$$

and

$$\kappa = \frac{k\rho\rho'}{\rho+\rho'} .$$

The value of $N^{\pm}$ is decided by the integer which most closely satisfies the equation

$$2nN^{\pm}\pi - \beta = \pm \pi.$$

Substituting Eqs. (A-21) and (A-23) into Eqs. (A-8) and (A-9), we obtain

(A-26a) $$G_b^p(\bar{\rho},\bar{\rho}') = g^p(\bar{\rho},\bar{\rho}';\beta^-) - g^p(\bar{\rho},\bar{\rho}';\beta^+)$$

(A-26b) $$G_b^d(\bar{\rho},\bar{\rho}') = g^d(\bar{\rho},\bar{\rho}';\beta^-) - g^d(\bar{\rho},\bar{\rho}';\beta^+)$$

and

(A-27a) $$W_a^p(\bar{\rho},\bar{\rho}') = g^p(\bar{\rho},\bar{\rho}';\beta^-) + g^p(\bar{\rho},\bar{\rho}';\beta^+)$$

(A-27b) $$W_a^d(\bar{\rho},\bar{\rho}') = g^d(\bar{\rho},\bar{\rho}';\beta^-) + g^d(\bar{\rho},\bar{\rho}';\beta^+)$$

where the superscript p denoted the contribution from pole singularities; the superscript d, from the saddle points.

Equations (11a) and (13b) have been evaluated in the same manner by Pathak and Kouyoumjian[20], in which G_a and W_b are given as

(A-28a) $$G_a^p(\bar{\rho},\bar{\rho}') = I^p(\bar{\rho},\bar{\rho}';\beta^-) - I^p(\bar{\rho},\bar{\rho}';\beta^+)$$

(A-28b) $$G_a^d(\bar{\rho},\bar{\rho}') = I^d(\bar{\rho},\bar{\rho}';\beta^-) - I^d(\bar{\rho},\bar{\rho}';\beta^+)$$

and

(A-29a) $$W_b^p(\bar{\rho},\bar{\rho}') = I^p(\bar{\rho},\bar{\rho}';\beta^-) + I^p(\bar{\rho},\bar{\rho}';\beta^+)$$

(A-29b) $$W_b^d(\bar{\rho},\bar{\rho}') = I^d(\bar{\rho},\bar{\rho}';\beta^-) + I^d(\bar{\rho},\bar{\rho}';\beta^+)$$

where

$$(A\text{-}30)\qquad I^{p}(\bar{\rho},\bar{\rho}';\beta) =$$

$$\sqrt{\frac{2}{j\pi k(\rho^2+\rho'^2-2\rho\rho'\cos\xi_p)^{1/2}}}\times e^{-jk(\rho^2+\rho'^2-2\rho\rho'\cos\xi_p)^{1/2}}\times$$

$$\times H[\pi-|-\beta+2nN\pi|],$$

and

$$(A\text{-}31)\qquad I^{d}(\bar{\rho},\bar{\rho}';\beta) \sim \left[-\frac{j}{4}\sqrt{\frac{2j}{\pi k\rho'}}\,e^{-jk\rho'}\right] d\,\frac{e^{-jk\rho}}{\sqrt{\rho}}$$

with

$$(A\text{-}32)\qquad d(\beta) = -\frac{e^{-j\frac{\pi}{4}}}{2n\sqrt{2\pi k}}\left[\cot\left(\frac{\pi+\beta}{2n}\right)F[\kappa a^{+}(\beta)] + \cot\left(\frac{\pi-\beta}{2n}\right)F[\kappa a^{-}(\beta)]\right].$$

The superscripts p and d of $I(\bar{\rho},\bar{\rho}';\beta)$ denote the contributions from pole singularities and saddle points, respectively.

Now, let us consider the pole singularity contribution for the case N = 0 and $\beta^{-} = \phi-\phi'$. The equation $|\phi-\phi'|<\pi$, i.e., $\phi<\pi+\phi'$, describes an illuminated region for a cylindrical wave illumination on a wedge (see Fig. 3). The spatial factor

$$\frac{e^{-jk\sqrt{\rho^2+\rho'^2-2\rho\rho'\cos(\phi-\phi')}}}{\sqrt{\rho^2+\rho'^2-2\rho\rho'\cos(\phi-\phi')}}$$

indicates that this pole singularity contribution yields the incident field. Thus, substituting Eqs. (A-26a), (A-27a), (A-28a), and (A-29a) into Eq. (A-4) and recognizing that U is the incident field,

$$-\frac{j}{4}\frac{2j}{\pi k\rho'}e^{-jk\sqrt{|\rho-\rho'|}}$$

we obtain

$$C = 1.$$

Therefore Eq. (A-4) becomes

$$(A\text{-}33)\qquad U_{\substack{a\\b}}(\bar{\rho},\bar{\rho}') \sim \frac{\lambda_{\substack{a\\b}} G_{\substack{a\\b}} - jk\sin\phi W_{\substack{a\\b}}}{\lambda_{\substack{a\\b}} - jk\sin\phi} \quad .$$

The above inference can be reverified by considering the reflected field, which is obtained from the pole singularity corresponding to the case N = 0 and $\beta^+ = \phi+\phi'$, we obtain

$$(A\text{-}34)\qquad U^p_{\substack{a\\b}} = \frac{jk\sin\phi+\lambda_{\substack{a\\b}}}{jk\sin\phi-\lambda_{\substack{a\\b}}} \left[-\frac{j}{4}\sqrt{\frac{2j}{\pi k(\rho^2+\rho'^2-2\rho\rho'\cos(\phi+\phi'))^{1/2}}}\right] x$$

$$x\, e^{-jk(\rho^2+\rho'^2-2\rho\rho'\cos(\phi-\phi'))^{1/2}} \quad ,$$

which is the reflected field from the reactance surface, ϕ=0. Whereas for the case N=1, $\beta=\phi+\phi'$,

$$(A\text{-}35)\qquad U^p_{\substack{a\\b}}(\bar{\rho},\bar{\rho}') =$$

$$\begin{bmatrix}-1\\1\end{bmatrix}\left[-\frac{j}{4}\frac{2j}{\pi k\left(\rho^2+\rho'^2-2\rho\rho'\cos(2n\pi-(\phi+\phi'))\right)^{1/2}}\right] x$$

$$x\, e^{-jk\left(\rho^2+\rho'^2-2\rho\rho'\cos(2n\pi-(\phi+\phi'))\right)^{1/2}}$$

is the reflected field from the perfectly-conducting surface, $\phi=n\pi$.

The diffracted field component is then obtained from the saddle point contributions to the function G and W, which is given in the form of

$$(A\text{-}36) \qquad U_{a\,b}^{d}(\bar{\rho},\bar{\rho}') \sim U^{i}\, D_{a\,b}\, \frac{e^{-jk\rho}}{\sqrt{\rho}} \quad ,$$

where

$$U^{i} \sim -\frac{j}{4}\sqrt{\frac{2j}{\pi k\rho'}}\; e^{-jk\rho'}$$

$$(A\text{-}37a) \qquad D_{a} = \frac{\lambda_a D_s - jk\sin\phi D_{g1}}{\lambda_a - jk\sin\phi}$$

$$(A\text{-}37b) \qquad D_{b} = \frac{\lambda_b D_{g2} - jk\sin\phi D_{h}}{\lambda_b - jk\sin\phi} \quad ,$$

with

$$D_{s\,h} = d(\beta^{-}) \mp d(\beta^{+})$$

and

$$D_{g1\,g2} = d_g(\beta^{-}) \pm d_g(\beta^{+}) \quad .$$

B. Plane Wave Illumination

The result for the plane wave case can be obtained by letting $\rho' \to \infty$ in the line source case of the last section A so that $\frac{k\rho\rho'}{\rho+\rho'} \to k\rho$ in the expression for κ. However, for the sake of completeness, we shall treat this problem by starting from Eq. (A-5) in which ρ and ρ' are interchanged. In this case, $k\rho' >> k\rho$. Thus, instead of the approximation made in Eq. (A-16), we have

$$(A\text{-}38) \qquad K_0(jkZ(\xi)) \sim \left[-\frac{j}{4}\sqrt{\frac{2j}{\pi k\rho'}}\, e^{-jk\rho'} \right] 2\pi\, e^{jk\rho\cos\xi}$$

which is given in Reference [16]. Therefore Eq. (A-18) becomes

$$(A\text{-}39) \qquad g(\bar{\rho},\bar{\rho}';\beta) \sim \left[-\frac{j}{4}\sqrt{\frac{2j}{\pi k\rho'}}\, e^{-jk\rho'} \right] \int_{L-L'} F_1(\xi,\beta)\, e^{jk\rho\cos\xi}\, d\xi \,.$$

Eliminating the "line source factor" appearing in the bracket and proceeding in a manner similar to that of part A for cylindrical wave illumination, we obtain

$$(A\text{-}40a) \qquad g^p(\bar{\rho},\bar{\rho}';\beta) = e^{jk\rho\cos\xi_p} \cos N\pi \times H[\pi - |-\beta+2nN\pi|],$$

and

$$(A\text{-}40b) \qquad g^d(\bar{\rho},\bar{\rho}';\beta) \sim d_g \frac{e^{-jk\rho}}{\sqrt{\rho}}$$

where d_g is identical to Eq. (A-24) except $\kappa = k\rho$ in this case.

The asymptotic form for G_b and W_a are also given by Eqs. (A-26) and (A-27), respectively. G_a and W_b for the plane wave illumination are derived in the same way by Pathak and Kouyoumjian[20], in which they give

$$(A\text{-}41a) \qquad I^p(\bar{\rho},\bar{\rho}';\beta) = e^{jk\rho\cos\xi_p} H[\pi - |-\beta+2nN\pi|],$$

and

$$(A\text{-}41b) \qquad I^d(\bar{\rho},\bar{\rho}';\beta) \sim d \frac{e^{-jk\rho}}{\sqrt{\rho}}$$

where d is the same as those given in Eq. (A-32) except the large parameter, $\frac{k\rho\rho'}{\rho+\rho'}$, replace by $k\rho$. G_a^p and G_a^d are still given by Eqs. (A-28) and (A-29).

In summary, plane wave illumination on a wedge is a special case of cylindrical wave illumination. The diffracted field component for plane wave illumination is thus still given as

$$(A\text{-}42) \qquad U_{\substack{a\\b}}^{d}(\bar{\rho},\bar{\rho}') \sim U^{i}(Q_E)\, D_{\substack{a\\b}}\, \frac{e^{-jk\rho}}{\sqrt{\rho}}\,,$$

where $D_{\substack{a\\b}}$ are given in Eqs. (A-37a) and (A-37b) with the large parameter $\frac{k\rho\rho'}{\rho+\rho'}$ replaced by $k\rho$. The reflection coefficient R is given as

$$(A\text{-}43) \qquad R = \begin{cases} 1 \\ -1 \\ \dfrac{jk\sin\phi+\lambda}{jk\sin\phi-\lambda} \end{cases}$$

which depends on the boundary condition at the surface of reflection.

C. Spherical Wave Illumination

Consider a scattering field $U_{\substack{a\\b}}(\bar{s},\bar{s}')$ which satisfies the wave equation

$$(A\text{-}44) \qquad (\nabla^2+k^2)\, U_{\substack{a\\b}}(\bar{s},\bar{s}') = -\,\delta(x-x')\,\delta(y-y')\,\delta(z-z'),$$

and the boundary conditions (2), (4) and Meixner edge condition, U_a satisfies Eq. (3a); U_b, Eq. (3b). Fourier transforming Eq. (A-44) yields

$$(A\text{-}45) \qquad (\nabla_t^2+k_t^2)\, \tilde{U}_{\substack{a\\b}}(\rho,\phi,h;\rho',\phi',z') = -\,\delta(x-x')\,\delta(y-y')\, e^{-jhz'}$$

where $U_{\substack{a\\b}}$ and $\tilde{U}_{\substack{a\\b}}$ are a Fourier transform pair given in Eqs. (34) and (35), and $k_t^2 = k^2 - h^2$. Equation (A-45) can be rewritten as

(A-46) $$(\nabla_t^2+k_t^2)\,\tilde{U}_{\substack{a\\b}}(\rho,\phi,h;\rho',\phi',z')\,e^{jhz'} = -\,\delta(x-x')\,\delta(y-y')$$

which is identical to Eq. (A-1) with the exception that k is replaced by k_t in Eq. (A-1). Thus

(A-47) $$(\frac{\partial}{\partial y}+\lambda)\tilde{U}_{\substack{a\\b}}\,e^{jhz'} = [(C-1)\frac{\partial}{\partial y'}+\lambda]\tilde{G}_{\substack{a\\b}}(\bar{\rho},\bar{\rho}';k_t) + \frac{\partial}{\partial y}\tilde{W}_{\substack{a\\b}}(\bar{\rho},\bar{\rho}';k_t)$$

where

(A-48a) $$\begin{bmatrix}\tilde{G}_a\\ \tilde{W}_b\end{bmatrix} = \tilde{\Upsilon}(\bar{\rho},\bar{\rho}';\beta^-,k_t) \mp \tilde{\Upsilon}(\bar{\rho},\bar{\rho}';\beta^+,k_t)$$

and

(A-48b) $$\begin{bmatrix}\tilde{G}_b\\ \tilde{W}_a\end{bmatrix} = \tilde{g}(\bar{\rho},\bar{\rho}';\beta^-,k_t) \mp \tilde{g}(\bar{\rho},\bar{\rho}';\beta^+,k_t)$$

with

(A-49a) $$\tilde{g}(\bar{\rho},\bar{\rho}',\beta,k_t) = \frac{1}{8\pi^2 nj}\int_{L-L'}\left[\frac{\cos^2(\frac{\xi+\beta}{2n})}{\sin(\frac{\xi+\beta}{2n})} + \sin(\frac{\xi+\beta}{2n})\right] K_o(jZ(\xi))d\xi$$

and

(A-49b) $$\tilde{\Upsilon}(\bar{\rho},\bar{\rho}';\beta,k_t) = \frac{1}{8\pi^2 nj}\int_{L-L'}\cot(\frac{\xi+\beta}{2n})\,K_o(jZ(\xi))d\xi$$

$Z(\xi)$ is given as $k_t\sqrt{\rho^2+\rho'^2-2\rho\rho'\cos\xi}$.

From the inverse Fourier transform relation and the approximation, $\frac{\partial}{\partial y} \sim -jk\sin\phi$, made in the far zone, Eq. (A-47) becomes

$$(A\text{-}50)\qquad U_{\underset{b}{a}}(\bar{s},\bar{s}') \sim \frac{[(C-1)\frac{\partial}{\partial y'} + \lambda]\, G_{\underset{b}{a}} - jkc\sin\phi W_{\underset{b}{a}}}{\lambda - jk\sin\phi}$$

$G_{\underset{b}{a}}$ and $W_{\underset{b}{a}}$ can be written as

$$(A\text{-}51a)\qquad \begin{bmatrix} G_a \\ W_b \end{bmatrix} = I(\bar{\rho},z;\bar{\rho}',z';\beta^-) \mp I(\bar{\rho},z;\bar{\rho}',z';\beta^+)$$

and

$$(A\text{-}51b)\qquad \begin{bmatrix} G_b \\ W_a \end{bmatrix} = g(\bar{\rho},z;\bar{\rho}',z';\beta^-) \mp g(\bar{\rho},z;\bar{\rho}',z';\beta^+)$$

where

$$(A\text{-}52a)\qquad I(\bar{\rho},z;\bar{\rho}',z';\beta) =$$

$$\frac{1}{2\pi}\int_{-\infty}^{\infty}\left[\int_{L-L'}\frac{1}{8\pi^2 jn}\cot\left(\frac{\xi+\beta}{2n}\right)K_o(jZ(\xi))e^{-jh(z'-z)}\,d\xi\right]dh,$$

and

(A-52b)

$$g(\bar{\rho},z;\bar{\rho}',z';\beta) =$$

$$\frac{1}{2\pi}\int_{-\infty}^{\infty}\left[\int_{L-L'}\frac{1}{8\pi^2 jn}\left(\frac{\cos^2\left(\frac{\xi+\beta}{2n}\right)}{\sin\left(\frac{\xi+\beta}{2n}\right)} + \sin\left(\frac{\xi+\beta}{2n}\right)\right)K_o(jZ(\xi))e^{-jh(z'-z)}d\xi\right]dh.$$

By utilizing

$$(A\text{-}53)\qquad K_\nu(jZ) = -j\,\frac{\pi}{2}\,e^{-j\nu\frac{\pi}{2}}\,H_\nu^{(2)}(z)$$

and[4]

$$(A\text{-}54)\qquad \int_{-\infty}^{\infty} dh\; H_0^{(2)}\left(\sqrt{k^2-h^2}\left\{\rho^2+\rho'^2-2\rho\rho'\cos\xi\right\}^{1/2}\right) e^{-jh(z'-z)}$$

$$\equiv 2j\,\frac{e^{-jk\sqrt{\rho^2+\rho'^2-2\rho\rho'\cos\xi+(z-z')^2}}}{\sqrt{\rho^2+\rho'^2-2\rho\rho'\cos\xi+(z-z')^2}}$$

Equation (A-52b) becomes

$$(A\text{-}55)\qquad g(\bar{\rho},z;\bar{\rho}',z',\beta) =$$

$$\int_{L-L'} F_1(\xi,\beta)\,\frac{e^{-jk\sqrt{\rho^2+\rho'^2-2\rho\rho'\cos\xi+(z-z')^2}}}{4\pi\sqrt{\rho^2+\rho'^2-2\rho\rho'\cos\xi+(z-z')^2}}\,d\xi$$

where $F_1(\xi,\beta)$ is given in Eq. (A-19a).

Note $\rho=s\sin\beta_o$ and $\rho'=s'\sin\beta_o$ (see Fig. 4). Hence $|(Z-Z')|^{1/2} = (s+s')\cos\beta_o$, and

$$(A\text{-}56)\qquad \rho^2+\rho'^2-2\rho\rho'\cos\xi+(z-z')^2 = (s+s')^2\left[1-\frac{2ss'\sin^2\beta_o}{(s+s')^2}\;x\;x\;(1+\cos\xi)\right]$$

Substituting the above equations in Eq. (A-55) yields

$$(A\text{-}57)\qquad g(\bar{\rho},z;\bar{\rho}',z';\beta) =$$

$$\int_{L-L'} d\xi\; F_1(\xi,\beta)\,\frac{e^{-jk(s+s')\sqrt{1-\frac{2ss'\sin^2\beta_o}{(s+s')^2}(1+\cos\xi)}}}{4\pi\sqrt{(s+s')^2-2ss'\sin^2\beta_o(1+\cos\xi)}}$$

As before, the integral over L-L' is evaluated asymptotically for large $\frac{kss'}{s+s'}\sin^2\beta_o$, and the SDP ($\pm\pi$) and L-L' form a closed contour which allows us to use the Cauchy Residue Theorem. The pole singularities contribution yields

$$(A\text{-}58)\qquad g^p = \frac{1}{4\pi}\,\frac{e^{-jk(s+s')\sqrt{1-\frac{2ss'\sin^2\beta_o}{(s+s')^2}(1+\cos\xi_p)}}}{\sqrt{(s+s')^2-2ss'\sin^2\beta_o(1+\cos\xi_p)}}\cos N\pi \;\; x$$

$$x\; H(\pi-|-\beta+2nN\pi|),$$

where

$$\xi_p = -\beta + 2nN \quad , \quad N = 0, 1, 2, \cdots$$

and $$|\xi_p| < \pi \; .$$

By making the following approximation

$$(A\text{-}59)\qquad e^{-jk(s+s')\sqrt{1-\frac{2ss'\sin^2\beta_o}{(s+s')^2}(1+\cos\xi)}}$$

$$\sim e^{-jk(s+s')\left\{1-\frac{ss'\sin^2\beta_o}{(s+s')^2}(1+\cos\xi)\right\}} \; ,$$

the saddle point contributions to Eq. (A-57) can be obtained in a manner similar to that for cylindrical wave illumination. Thus

$$(A\text{-}60)\qquad g^d \sim \left[\frac{1}{4\pi}\,\frac{e^{-jks'}}{s'}\right] d_g \sqrt{\frac{s'}{s(s+s')}}\, e^{-jks}$$

where d_g is given in Eq. (A-24) with the exception that $\kappa = \frac{kss'}{s+s'}\sin^2\beta_o$ in this case.

The integral $I(\bar{\rho},z;\bar{\rho}',z';\beta)$ is evaluated in the same way by Pathak and Kouyoumjian[20]. Combining all the results we got thus far, and recognizing that the pole contribution for the case N = 0, $\beta = \phi-\phi'$ yields the direct incident field, we can determine that

$$C = 1.$$

Thus the diffracted field component of $U_{\substack{a\\b}}^{d}(\bar{s},\bar{s}')$ can be written as

$$U_{\substack{a\\b}}^{d}(\bar{s},\bar{s}') \sim U^{i} D_{\substack{a\\b}} \sqrt{\frac{s'}{s(s+s')}}\, e^{-jks} \tag{A-61}$$

where $D_{\substack{a\\b}}$ are given in Eqs. (A-37a) and (A-37b) with the large parameter $\kappa = \frac{kss'}{s+s'} \sin^2\beta_o$, and

$$U^{i} \sim \frac{e^{-jks'}}{4\pi s'} .$$

REFERENCES

1. Chu, T.S., "Surface Wave Diffraction and Its Relationship to Surface Wave Antennas," Ph.D. Dissertation, The Ohio State University ElectroScience Laboratory, Department of Electrical Engineering, 1960.

2. Chu, T.S., Kouyoumjian, R.G., Karal, F.C., and Karp, S.N., "The Diffraction of Surface Waves by a Terminated Structure in the Form of a Right-angled Bend," IEEE Trans. on Antenna and Propagation, Vol. AP-10, No. 6, November 1962.

3. Felson, L.B., "Field Solution for a Class of Corrugated Wedge and Cone Surfaces," Polytechnic Institute of Brooklyn, Microwave Res. Inst., Tech. Memo., No. 32, July 1957.

4. Harrington, R.F., Time Harmonic Electromagnetic Fields, New York, McGraw-Hill, 1961, Chapters V and VI.

5. Hutchins, D.L. and Kouyoumjian, R.G., "Asymptotic Series Describing the Diffraction of a Plane Wave by a Wedge," Report 2183-3, 15 December 1969, The Ohio State University ElectroScience Laboratory, Department of Electrical Engineering; prepared under Contract AF 19(628)-5929 for Air Force Systems Command. (AD 699 228)(AFCRL-69-0412). (See also: Hutchins, D.L. and Kouyoumjian, R.G., "A New Asymptotic Solution to the Diffraction by a Wedge," URSI Spring Meeting, Ottawa, Canada, 1967.)

6. Hwang, Y.M., Kouyoumjian, R.G. and Pathak, P., "The Radiation from Slots in Truncated, Dielectric-covered Surfaces," 1971 G-AP International Symposium, Los Angeles, California, September 1971.

7. Karal, F.C. and Karp, S.N., "Diffraction of a Plane Wave by a Right Angled Wedge Which Sustains Surface Waves on One Surface," New York University, Inst. Math. Sci., Div. Electromagnetic Res., Res. Rep. EM-123, 1959.

8. Karal, F.C., Karp, S.N., Chu, T.S. and Kouyoumjian, R.G., "Scattering of a Surface Wave by a Discontinuity in the Surface Reactance on a Right-angled Wedge," Commun. Pure Appl. Math., Vol. 14, February 1961, pp. 35-48.

9. Karp, S.N. and Karal, F.C., "Vertex Excited Surface Waves on One Face of a Right Angle Wedge," New York Univ., Inst. Math. Sci., Div. Electromagnetic Res., Res. Rep. EM-124, 1959.

10. Karp, S.N., "Two Dimensional Green's Function for a Right Angled Wedge Under an Impedance Boundary Condition," Commu. on Pure and Appl. Math., Vol. XIII, 1960, pp. 203-216.

11. Karp, S.N. and Karal, F.C., Jr., "Generalized Impedance Boundary Conditions with Applications to Surface Wave Structures," EM wave Theory Proceedings of a Symp. held at Delft, The Netherlands, September 1965.

12. Keller, J.B., "Geometrical Theory of Diffraction," Journal of the Optical Society of America, Vol. 52, February 1962, pp. 116-130.

13. Kouyoumjian, R.G., "Asymptotic High-Frequency Methods," Proceedings of IEEE, Vol. 53, No. 8, August 1965, pp. 864-876.

14. Kouyoumjian, R.G. and Pathak, P., "The Dyadic Diffraction Coefficient for a Perfectly Conducting Edge Structure," presented at URSI Fall Meeting, Los Angeles, California, 1971.

15. Lewy, H., "Waves on Sloping Beaches," Bull. Amer. Math. Soc., Vol. 52, 1946, pp. 737-773.

16. MacDonald, H.M., Electric Waves, Cambridge University, Press, Cambridge, 1902, pp. 186-198.

17. Malyughinets, G.D., Dokl. Akad. Nauk SSSR, 121, No. 3, 1958, p. 436.

18. Malyughinets, G.D., Annalen der Physik, 6, No. 1-2, 1960, pp. 107-112.

19. Mohsen, A. and Hamid, M.A.K., "Diffraction by a Dielectric-loaded Wedge," Radio Science, Vol. 8, No. 1, January 1973, pp. 71-80.

20. Pathak, P. and Kouyoumjian, R.G., "The Dyadic Diffraction Coefficient for a Perfectly-conducting Wedge," Report 2183-4, 5 June 1970, The Ohio State University ElectroScience Laboratory, Department of Electrical Engineering; prepared under Contract AF 19(628)-5929 for Air Force Systems Command. (AFCRL-69-0546)

21. Peters, A.S., "Water Waves over Sloping Beaches and the Solution of a Mixed Boundary Valve Problem for $(\Delta^2 - k^2)\phi = 0$ in a Sector," Commu. on Pure and Appl. Math., 5, 1952, pp. 87-108.

22. Senior, T.B.A., "Diffraction by an Imperfectly Conducting Wedge," Commu. on Pure and Appl. Math., 12, 1959, pp. 337-372.

23. Senior, T.B.A., "Impedance Boundary Conditions for Statistically Rough Surfaces," Appl. Sci. Res., Section B, Vol. 8, 1961, pp. 437-462.

24. Stoker, J.J., "Surface Waves in Water of Variable Depth," Quart. Appl. Math., Vol. 5, 1947, pp. 1-54.

☆ U.S. GOVERNMENT PRINTING OFFICE: 1974—739-160/122

"The aeronautical and space activities of the United States shall be conducted so as to contribute . . . to the expansion of human knowledge of phenomena in the atmosphere and space. The Administration shall provide for the widest practicable and appropriate dissemination of information concerning its activities and the results thereof."

—NATIONAL AERONAUTICS AND SPACE ACT OF 1958

NASA SCIENTIFIC AND TECHNICAL PUBLICATIONS

TECHNICAL REPORTS. Scientific and technical information considered important, complete, and a lasting contribution to existing knowledge.

TECHNICAL NOTES: Information less broad in scope but nevertheless of importance as a contribution to existing knowledge.

TECHNICAL MEMORANDUMS: Information receiving limited distribution because of preliminary data, security classification, or other reasons. Also includes conference proceedings with either limited or unlimited distribution.

CONTRACTOR REPORTS: Scientific and technical information generated under a NASA contract or grant and considered an important contribution to existing knowledge.

TECHNICAL TRANSLATIONS: Information published in a foreign language considered to merit NASA distribution in English.

SPECIAL PUBLICATIONS: Information derived from or of value to NASA activities. Publications include final reports of major projects, monographs, data compilations, handbooks, sourcebooks, and special bibliographies.

TECHNOLOGY UTILIZATION PUBLICATIONS: Information on technology used by NASA that may be of particular interest in commercial and other non-aerospace applications. Publications include Tech Briefs, Technology Utilization Reports and Technology Surveys.

Details on the availability of these publications may be obtained from:

SCIENTIFIC AND TECHNICAL INFORMATION OFFICE

NATIONAL AERONAUTICS AND SPACE ADMINISTRATION

Washington, D.C. 20546